# A THEORETICAL STUDY ON THE INTERACTION OF BIMETALLIC Pt-Ni SURFACE AND THE REACTANTS OF OXIDATIVE STEAM REFORMING REACTION

by

Elif Ercan

B. S. in ChE., Yeditepe University, 2006

Submitted to the Institute for Graduate Studies in
Science and Engineering in partial fulfillment of
the requirements for the degree of
Master of Science

Graduate Program in Chemical Engineering

Boğaziçi University

2009

***to my father***

# ACKNOWLEDGEMENTS

Firstly, I would like to express my thanks to my thesis supervisor, Prof. Ahmet Erhan Aksoylu, for his suggestions, comments and support throughout this study. I am grateful to him for his help in finding solutions to the problems.

I have special thanks to Aslıhan Sümer because of her great help and brightness; she has a great lovable character and she answered my everlasting questions with great patience. This study would never end without her help.

I am very grateful to my close friend; F. Banu Yavuztürk; she was my partner both in Yeditepe and Boğaziçi. I could not have graduated from anywhere without her. I also wish to thank to my friends in CATREL group; Feyza Gökaliler, Tuğba Davran Candan, Burcu Selen Çağlayan; they encouraged me when I was depressed. Also special thanks to the citizens of our lab; my dear friends; Sabriye Güven, İlker Öztürk and Görkem Oğur; they accompanied me, they made me smile all the time I was around here.

I would also like to thank my childhood friends; Şebnem Demirci and Zeynep Mersinoğlu; they were always by my side when I needed. Also I have grateful thanks to my friends, especially Fırat Ada; for his support and advices, to Gülçin Ergül; for her joyful character and online support. I thank to my all friends at Boğaziçi University, especially Ezgi Akkaya, Yasemen Güngörmez and Pınar Kanlıkılıçer, for their frienship and being full of joy.

Thanks to my mother Nevin Ercan for her patience and love, to my father Şener Ercan for being a super-hero-dad, to my sister Hilal Ercan for encouraging me although there were kilometers between us for two years, and especially to my sister; G. İrem Ercan for her lively character and high energy even though she was under stress because of her big exam after middle school graduation; that young girl is my little princess.

This study is financially supported by Site Planning Organization of Turkey, DPT, through project DPT-07K120630, by TÜBİTAK through project 105M282 and by Boğaziçi University through a matching project 09M104.

# ABSTRACT

## A THEORETICAL STUDY ON THE INTERACTION OF BIMETALLIC Pt-Ni SURFACE AND THE REACTANTS OF OXIDATIVE STEAM REFORMING REACTION

Pt-Ni bimetallic system is an efficient catalyst for Oxidative Steam Reforming (OSR) reaction; the detailed experimental test results obtained from Pt-Ni system have been already given in literature. In those research papers, the importance of understanding the bimetallic surface properties and the interaction between active sites and OSR reactants has been mentioned.

In the current study (i) the properties of several bimetallic alloy surfaces having different Pt/Ni ratio, pseudomorphic Pt layers formed on Ni sublayers and monometallic Pt and Ni surfaces have been determined, (ii) the adsorption properties of all possible monometallic and bimetallic sites for oxygen and methane have been studied and (iii) the electronic interaction between metal atoms of the active sites and OSR reactant have been analyzed. The results showed that, Pt addition to Ni decreases the surface stress and the most stable site is found as 'five Ni layers containing 25 per cent Pt at topmost layer' surface alloy based on surface energy calculations. The adsorption studies indicate that oxygen adsorption energy does not only depend on surface concentrations of Pt and Ni but also the number of Pt-O and Ni-O bonds on the fcc site. Additionally, it was found that surface stress may be an important parameter in adsorption properties of the surface.

# ÖZET

## ÇİFT METALLİ Pt-Ni YÜZEYİNİN VE OKSİDATİF BUHARLI REFORMLAMA TEPKİMESİNE KATILAN MADDELERİN ETKİLEŞİMLERİ ÜZERİNE TEORİK BİR ÇALIŞMA

Pt-Ni çift metalli sistem, Oksidatif Buharlı Reformlama (OBR) reaksiyonunda etkili bir katalizördür; Pt-Ni sisteminden elde edilen ayrıntılı deneysel test sonuçları literatürde önceden verilmiştir. Bu makalelerde, çift metalli yüzeyin özelliklerinin ve çift metalli yüzey ile OBR tepkimesine katılan maddelerin etkileşimlerinin anlaşılmasının önemine değinilmiştir.

Hali hazırdaki çalışmada (i) farklı miktarlarda Pt/Ni oranına sahip birçok çift metalli alaşım yüzeylerinin özellikleri, Ni alt katmanları üzerinde oluşmuş psodomörf Pt katmanları ve monometalik Pt ve Ni yüzeyleri için, belirlenmiş, (ii) tüm olası monometalik ve bimetalik bölgelerin oksijen ve metan için adsorpsiyon özellikleri çalışılmış, (iii) aktif bölgelerdeki metal atomları ile OBR tepkimesine katılan maddeler arasındaki elektronik etkileşim analiz edilmiştir. Sonuçlar, Ni yüzeylerine Pt ilavesinin yüzey stresini azalttığını ve en kararlı durumun "en üst katmanında yüzde 25 Pt bulunduran 5 katmanlı Ni" yüzey alaşımı olduğunu yüzey enerji hesaplarına dayanarak göstermiştir. Adsorpsiyon çalışmaları, oksijen adsorpsiyon enerjisinin sadece Pt ve Ni yüzey konsantrasyonuna bağlı olmadığını, aynı zamanda fcc bölgesindeki Pt-O ve Ni-O bağ sayısına da bağlı olduğunu göstermiştir. Bunun yanı sıra, yüzey stresinin yüzeydeki adsorpsiyon özellikleriyle ilgili önemli bir parametre olabileceği vurgulanmıştır.

# TABLE OF CONTENTS

# LIST OF FIGURES

# LIST OF TABLES

# LIST OF ABBREVIATIONS

| | |
|---|---|
| ATR | Autothermal reforming |
| $C/O_2$ | Carbon to oxygen ratio |
| DFT | Density functional theory |
| GGA | Generalized gradient approximation |
| $H_2/CO$ | $H_2$ selectivity |
| IPOX | Indirect partial oxidation |
| LDOS | Local density of states |
| OSR | Oxidative steam reforming, |
| PEMFC | Proton exchange membrane fuel cell |
| PBE | Perdew-Burke-Ernzerhof |
| PROX | Preferential oxidation |
| SCF | Self-consistent field |
| SR | Steam reforming |
| S/C | Steam to carbon ratio |
| TOX | Total oxidation |
| WGS | Water-gas shift |
| W/F | Residence time |

# 1. INTRODUCTION

The depletion of fossil based energy sources and the climate change that have resulted from the case of conventional routes in energy production impose the improvement of new technologies for energy production. Fuel cell; an electrochemical device where a fuel reacts with oxygen for generating electricity is one of the best alternative options for substitution to fossil fuel-based conventional energy production systems. [1-4]

Among different types of fuel cells, the proton exchange membrane fuel cell (PEMFC) fuelled by hydrogen seems to be the most promising alternative for small scale and vehicular systems. As there are technological obstacles for hydrogen storage and no available hydrogen distribution network, on site production of CO-free hydrogen to be used as a feed to PEMFC and using fuel processors is a promising option. In a fuel processor, three main catalytic reactions occur in series; reforming, water-gas shift (WGS) and preferential oxidation (PROX). [5, 6]

In a fuel processor, many different types of reforming reactions can be conducted; *Oxidative Steam Reforming (*OSR) is one of these reactions via which hydrogen is produced by hydrocarbon fuels. OSR is a combination of steam reforming (SR) and total oxidation (TOX), in which endothermic SR reaction absorbs the heat released from exothermic TOX reaction. The reports of the experiments conducted on bimetallic Pt-Ni/δ-$Al_2O_3$ catalyst system in literature indicate that Pt-Ni bimetallic system is an efficient OSR catalyst; in Pt-Ni system, the catalyst particles act like micro heat exchangers, supply heat produced on TOX (Pt) sites to SR (Ni) sites. [7]

In the current study (i) the properties of several bimetallic alloy surfaces having different Pt/Ni ratio, pseudomorphic Pt layers formed on Ni sublayers and monometallic Pt and Ni surfaces have been determined, (ii) the adsorption properties of all possible monometallic and bimetallic sites for oxygen and methane have been studied and (iii) the electronic interaction between metal atoms of the active sites and OSR reactant have been analyzed.

In the current study, (i) the possible adsorption sites for O and $CH_4$ on Ni were found from the literature within the previous Quantum Mechanical simulation studies and also checked by CASTEP calculations among this study. (ii) Since the adsorption energy calculations require clean surface energy data, the surface energies of possible clean surfaces were calculated and compared. Then the relationship between stability of surfaces and surface stress were investigated. (iii) The adsorption energies and geometries of the adsorbates were calculated on theoretically specified sites. (iv) The comparisons of the adsorption energies of adsorbates for the same sites on surfaces with different Pt and Ni concentrations were made. (v) The effects of number of Pt-O and Ni-O bond on adsorption energies were investigated. (vi) In OSR reaction; $CH_4$, O, $H_2O$ are the reactants; since $CH_4$ is common in both Pt and Ni sites, adsorption of oxygen has a key role for specifying the oxidation site which was assumed to be mainly on the Pt sites.

In the report, Chapter 2 gives general information about the fuel cells, previous OSR reaction studies and catalysts used in OSR reactions. Moreover the effect of alloying on adsorption and previous computational studies on Ni and Pt-Ni surfaces will be considered. Computational work will be explained on Chapter 3 in details. The results will be discussed in the Chapter 4 and the conclusions of the work will be given in the Chapter 5.

# 2. LITERATURE SURVEY

## 2.1. Fuel Cell Technology

Fuel cell technology is one of the newest alternatives for clean energy production. Various types of fuel cells have been developed for both stationary and mobile power generation. Various hydrocarbons are reformed to produce CO-free hydorgen to be used as feed to fuel cells. [8-9]

The fuel cells are normally distinguished by the electrolyte that they contain. Alkaline, molten carbonate, phosphoric acid, proton exchange membrane and solid oxide fuel cells are the best known types. [10]

For small scale and transport applications, the most favorable fuel cell technology is the Proton Exchange Membrane Fuel Cell (PEMFC) which is powered by hydrogen. Hydrogen is split into its protons and electrons at the anode of the PEMFC. Then, protons move from the anode to the cathode through a membrane where the reaction that produces water takes place. Continuous supply of CO-free hydrogen is desired for PEMFC since even small amount of CO impurity leads to poisoning of Pt anode at the operation temperatures of the PEMFC. Increasing the operation temperature is not an option as the operation temperatures above 85 ºC leads the dehydration of the polymeric membrane. For producing CO-free hydrogen from various hydrocarbons, fuel processors, in which three catalytic reactions are conducted in series, are used. Those reactions are steam reforming (SR), water-gas shift (WGS), and preferential oxidation (PROX). Reforming reactions are used to produce hydrogen from hydrocarbons, WGS increases hydrogen concentration while decreases CO concentration in the stream, and the last reaction, PROX, eliminates CO impurity from the resultant hydrogen rich stream. [3, 5, 7, 8, 11-13] The main focus in this study is the investigation of the interaction between an efficient, bimetallic system that catalyzes OSR, Pt-Ni, and the reactants of OSR reaction, oxygen and methane.

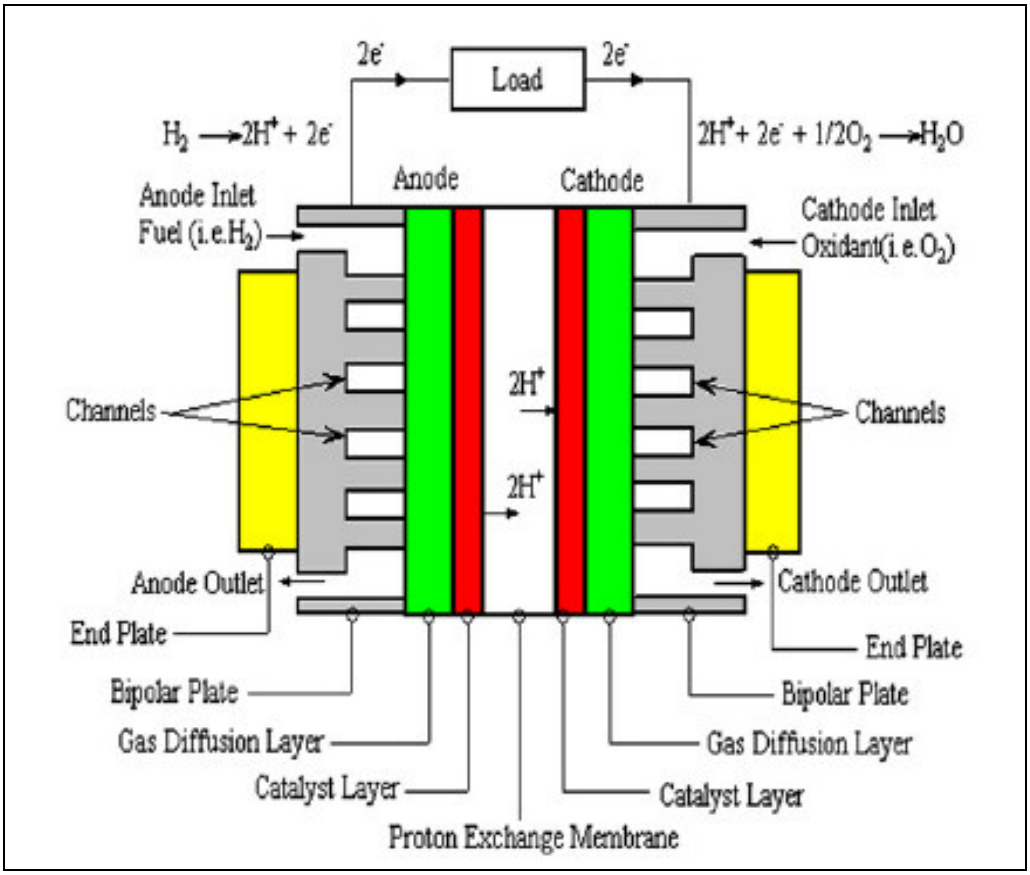


Figure 2.1. PEM Fuel Cell [1]

## 2.2. Oxidative Steam Reforming

One type of the reforming reactions conducted in a fuel processor is Oxidative Steam Reforming (which also has alternative names; Indirect Partial Oxidation -IPOX- or Autothermal Reforming -ATR-); OSR is combination of two main reactions; Steam Reforming (SR) and Total Oxidation (TOX), which are given below, respectively. [3, 7, 11-13]

$$\left.\begin{aligned} C_nH_m + nH_2O &\rightarrow nCO + (½m + n)H_2 \\ C_nH_m + (n + (¼)m)O_2 &\rightarrow nCO_2 + (½)mH_2O \end{aligned}\right\} \text{ OSR} \qquad (2.1)$$

## 2.3. Catalysts for OSR and Other Reforming Reactions

Considering the high cost and limited availability of noble metals, Ni is the widely accepted choice of active metal used in reforming catalysts. On the other hand, the studies revealed that, the presence of oxygen causes loss in the reforming activity of Ni species as they are oxidized during the reaction, especially at elevated temperatures. [14, 15]

Several effective OSR catalysts have been designed and tested in CATREL group. One of the most successful catalysts developed for OSR reactions by CATREL is Pt-Ni/$Al_2O_3$: there have been several experimental papers published in the literature offering OSR test results from Pt-Ni system. In OSR studies over Pt-Ni, methane, propane, butane and LPG are used as the hydrocarbon feed. According to the experimental findings, Pt sites mostly catalyze oxidation and Ni sites mostly catalyze steam reforming. Since Pt-Ni bimetallic catalyst has both Pt and Ni on the same support, the catalyst itself behaves as a heat exchanger at micro scale; the heat released by the exothermic TOX reaction occurs at Pt sites is transferred and used in the SR reaction catalyzed by Ni sites. As a result, high thermal efficiency is obtained during hydrogen production when bimetallic Pt-Ni system is used. [2, 4-7, 11-12]

In two experimental studies [6, 7] on OSR over Pt-Ni/$Al_2O_3$, the feeds used were propane and LPG which was composed of propane and n-butane. These feeds were sent onto bimetallic Pt-Ni catalyst supported on δ-$Al_2O_3$. During the experiments, effects of steam to carbon ratio (S/C), carbon to oxygen ratio (C/$O_2$) and residence time (W/F) on the hydrogen production activity, selectivity and product distribution were investigated [7]. In the first study, the results of the experiments showed that the bimetallic system has superior performance characteristics compared to the monometallic catalysts in the literature. High efficiency of Pt-Ni system stems from the fact that the bimetallic catalyst improves energy efficiency by utilizing the catalyst particles as micro heat exchangers during OSR; the heat which was obtained from exothermic TOX on Pt sites was used in the simultaneous SR reaction which was catalyzed by Ni sites. [6] In the second study it was shown that $H_2$ produced per mole of hydrocarbon feed ($H_2$ yield), $H_2$ selectivity ($H_2$/CO ratio in product) was increased when LPG was used as the feed compared to the use of pure propane as the feed. Based on these findings, it is claimed that Pt&Ni-LPG

system has a potential to be used in commercial fuel processors, which were designed for fuelling PEM fuel cells. [7]

In another study by Gökaliler et al. [4] LPG was used as the hydrocarbon feed in OSR tests conducted on bimetallic Pt-Ni/$Al_2O_3$. The experimental conditions were adjusted with the aim of determining the effect of S/C ratio and the propane/n-butane ratio in LPG feed on catalyst activity and selectivity. OSR tests were conducted over the bimetallic 0.2 wt.per cent Pt - 15 wt.per cent Ni/δ-$Al_2O_3$ catalyst for a feed having 1:1 propane:butane ratio between 623 K and 743 K. Although the thermodynamic calculations indicated the advantage of using low S/C ratio in the feed stream, the experiments showed that low S/C ratios made the catalyst surface prone to coke deposition and deactivation. Gökaliler et al. reported that the optimum residence time for high selectivity lied between the highest and the lowest applicable residence times, thus increasing the numerator ($H_2$ production) using low residence times or by decreasing the denominator (CO production) using high residence times had opposing effects. [4]

Steam reforming of n-butane over Ni/δ-$Al_2O_3$ and bimetallic Pt-Ni/δ-$Al_2O_3$ were studied between 578 K and 678 K by Avcı et al. The SR characteristics of both monometallic Ni and Pt and bimetallic Pt-Ni were compared under the same reaction conditions. At 648 K, Pt-Ni system showed superior activity in the $H_2$ selectivity which results from low amount of $CO_2$ and $CH_4$ formation. The major difference between Ni and Pt-Ni catalysts was observed in terms of temperature-activity relation; at 648 K; 100 per cent conversion of n-butane was obtained over Pt-Ni compared to 67 per cent conversion obtained over pure Ni. Based on these results, it was reported that; although monometallic Ni catalysts were the best steam reforming catalysts, they were not superior catalysts in OSR due to their limited TOX activity and their deactivation tendency through oxidation. Avcı et al. showed how the steam reforming characteristics of Ni were modified by the presence of Pt. The results of the study verified that, Ni was efficient in driving SR of hydrocarbons and Pt was efficient in the oxidation of them. [12]

Li et al. studied oxidative steam reforming of methane using Pt modified nickel catalysts. In the preparation of the catalysts, two methods, sequential impregnation and co-impregnation were used. They concluded that Pt-Ni bimetallic catalyst show high

resistance to hot spot formation. The results show that even small amount of Pt addition enhance the reduction properties and activity of the catalysts. [14]

In another study, Mukainakano et al. compared the catalytic activity of monometallic Ni and bimetallic Pt-Ni in OSR of methane. According to their results, the best performing catalyst was Pt(0.1)/Ni(2.6) which prevented the hot spot formation caused by temperature increase more effectively than other monometallic and bimetallic catalysts. Their CO adsorption studies utilizing EXAFS and FTIR showed that the Pt(0.1)/Ni(2.6) catalyst sample was highly reducible and this property of the catalyst was dependent on the properties of the active sites. High reducibility of the catalyst surface resulted in the overlap of two reaction zones, i.e. exothermic combustion reaction and endothermic reforming reaction, and by this way hot spot formation was presented. [16]

In another study, Yoshida et al. investigated the effect of Pd addition to Ni on the catalytic activity in OSR. It was shown that Pd-Ni bimetallic catalyst has the advantage of providing a more flat temperature profile in the reactor bed. [17] It is reported that, the catalytic performance and bed temperature profile on bimetallic catalysts in oxidative steam reforming of methane, were strongly influenced by the structure of bimetallic particles, whose extent is directly related with the relative atomic ratio of the metals on the surface. [14, 18-22]

Örücü et al. studied ethanol steam reforming between 673K and 823 K over Pt–Ni/δ-$Al_2O_3$. The optimum conditions were obtained around 773 K; at this temperature level both because of high hydrogen production rates and low CO and $CH_4$ production rates were obtained. In addition to that, higher water-to-ethanol ratios had a positive effect on both ethanol conversion and $H_2$ formation. [8]

Nikolla et al. assisted computational studies with experiments. They studied hydrocarbon SR on Ni alloys at solid oxide fuel cell operating conditions. They have found that; supported Sn/Ni is highly carbon tolerant and forming an alternative to Ni for catalytic hydrogen production from hydrocarbons through SR of isooctane at reasonable steam/carbon ratios. They showed that there were two reasons for that; high propensity of

Sn/Ni to oxidize carbon and lower driving force to form carbon deposits on low coordinated metal sites. [23]

## 2.4. Effect of Alloying on Adsorption

Alloying a metal with a second metal changes the electronic structure, and, consequently, the adsorptive properties of the surface. Considering that adsorption is the first step in many chemical reactions, it is meaningful to expect that alloys have different chemical activities than pure metals. There are many experimental and computational studies investigating the differences occurring in adsorption of the reactants and chemical activity on pure monometallic and bimetallic metal surfaces and catalysts.

Lischka et al. studied oxygen adsorption on pseudomorphic Pt/Ru bimetallic catalysts by using Density Functional Theory (DFT) calculations. They deposited Pt layer(s) on Ru layers; in their study, they started from depositing one layer Pt on four layers of Ru first and then increased the number of Pt layers. They found that when five layers of Pt were on Ru (top two layers of Ru and all the layers of Pt were relaxed), the most stable catalyst was obtained since it reduced both the atomic and the molecular adsorption energies of oxygen. Besides, they also found that with the increase in the Pt amount, the efficiency of the catalyst in cathodic oxygen reduction reaction was increased, too. [24]

Li et al. modified the Ni catalysts with Pt for oxidative steam reforming of methane by using two methods; sequential impregnation and co-impregnation. The study included the investigation of the modification effect of Pt based on the catalytic performance and catalyst bed temperature profile in the oxidative steam reforming of methane. They concluded that; when Pt was introduced to Ni catalyst through using sequential impregnation, catalytic performance had been improved and a flat bed temperature profile had been obtained. The improved performance of Pt-Ni bimetallic catalyst, especially the flat temperature profile, was related to oxygenation properties of the surface. The modification of Ni with Pt prevented the oxidation of Ni species near the bed inlet in the oxidative steam reforming of methane. On the contrary, monometallic Ni catalysts were oxidized under the same conditions. Lowered oxygenation property of Ni when alloyed

with Pt is led by the changes in its electronic structure through Pt-Ni electronic interaction. Additionally, Pt atoms preferred to be on the outer surface of the catalytic sites when the catalyst was prepared using sequential method. Presence of Pt on the surface also decreased the strength of oxygen adsorption on the surface. [14]

## 2.5. Computational Studies on Ni and Pt-Ni Surfaces

Some of the theoretical studies published by CATREL focused on the adsorption properties of bimetallic alloys using quantum mechanical calculations. Gülmen et al. and Sümer et al. studied the adsorption properties of CO on $Pt_3Sn$ and compared with the adsorption properties of monometallic Pt having the same geometry. In their series of papers, they mentioned that: (i) The comparison of CO adsorption on the Pt and $Pt_3Sn$ surface sites having the same geometry showed that Sn presence in the alloy limited the number of stable CO adsorption sites on the alloy surface and decreased CO adsorption. This is related with the fact that CO cannot adsorb on Sn. [25] (ii) Sümer et al. showed that there were significant differences between the electronic properties of Pt atoms at $Pt_3Sn$ surface and that of monometallic Pt, leading to changes in the CO bonding energies of these Pt atoms. The difference in adsorption strength of similar sites on these two surfaces was an apparent result of the difference in surface electronic structure. (iii) Low index and high index $Pt_3Sn$ surface terminations had different adsorption properties, because of the specific qualities of stepped structures compared to flat surfaces. [3].

Wang et al. reported on a theoretical study on the co-adsorption energies of reactants and subsequent reaction intermediates in $CO_2$ reforming of $CH_4$ over Ni(111) surface by using DFT calculations. The structures and energy barriers of the reactions were analyzed systematically, and a new mechanism has been proposed on the basis of the computed kinetic parameters of the elementary steps. The study involves reaction pathway analysis of $CO_2$ reforming of $CH_4$ on Ni (111). A new mechanism was obtained on the basis of the energy barriers. The first step of the mechanism was $CO_2$ dissociation into surface CO and O ($CO_2 \rightarrow CO + O$) and sequential $CH_4$ dissociation into surface to CH and hydrogen ($CH_4 \rightarrow CH_3 \rightarrow CH_2 \rightarrow CH$). The second step was CH oxygenation into CHO ($CH + O \rightarrow CHO$), which was more favored than its dissociation into C and hydrogen ($CH \rightarrow C + H$).

The third step was the dissociation of CHO into surface CO and H (CHO → CO + H). Finally, $H_2$ and CO desorbed from Ni (111) and formed free $H_2$ and CO. [26] The preferred $CH_4$ adsorption site in the current study is based on this paper.

Cabeza et al. studied the electronic and energetic properties of bimetallic surfaces using DFT calculations. Specifically, they aimed to study the structural and electronic properties of group VIII transition metals (TM) bimetallic systems. They deposited platinum on close packed surfaces of nickel and cobalt. They took four different systems into account: the pseudomorfic Pt/Ni(111) and Pt/Co(0001) overlayers, the normal Pt(111) surface and a fictive Pt(111) surface for which Pt atoms have the same interatomic distance with bulk Ni atoms. The chemical effect of replacing Pt atoms by another metal like Ni or Co was investigated. They have calculated the surface energies for pure metal surfaces and showed the ranking: Pt/Co > Co > Pt/Ni > Ni > Pt. They have concluded that, a smaller surface energy means a less reactive surface with low adhesion energy. [27]

Yamagashi et al. searched oxygen adsorption on Ni(111) in the $\left(\sqrt{3}x\sqrt{3}\right)$ unit cell using first-principles DFT studies. The structural and electronic properties of this system were investigated. The most stable adsorption was fcc site with an adsorption energy value as 4.21 eV per $O_2$ molecule (406 kJ/mol), which is in good agreement with the single crystal adsorption calorimeter value of 4.56 eV at 1/3 ML coverage. [28]

Sehested et al. researched on the effects of atmosphere and temperature on the rate of sintering of nickel steam-reforming catalysts, both experimentally and theoretically. They aimed to find the effects of steam and hydrogen over nickel catalysts as a function of temperature. Using the DFT calculations, it was summed up that, when there were steam and hydrogen, $Ni_2$–OH dimers dominated the surface transport at nickel particles. The calculated energies of formation and diffusion were used in a simple model that was able to estimate the rate of sintering of nickel catalysts. The estimated dependencies of temperature, $P_{H_2O}$, and $P_{H_2}$ were in agreement with those acquired experimentally. [15]

Ma et al. studied the surface segregation energy of platinum on a number of different $Pt_3M$ alloys and found that in these alloys Pt had a tendency to diffuse to the topmost surface layer from the bulk. This diffusion tendency is related to the surface energy and

atomic radius difference between Pt and the second metal; they found that the diffusion occurred when the system surface energy was energetically favorable and, additionally, when the atomic radius of the second metal was smaller than the radius of platinum. [29]

# 3. CALCULATIONS

## 3.1. Computational Details of CASTEP Calculations

Density functional calculations were performed in repeated slab geometry, using the program package CASTEP in Material Studio of Accelrys Inc. (version 4.4). The Pt-Ni surfaces were modeled as five-layer slabs, for which the atoms in the three bottom layers kept fixed in their bulk geometry, while the topmost two layers were relaxed. The vacuum thicknesses between the slabs were 12 Å. The electron-ion interactions were included through the use of ultra soft pseudo potentials and the electronic wave functions were expanded in a basis set of plane waves, up to kinetic energy cutoff of 300 eV. The convergence with respect to cutoff value was checked by using 400 eV; it was seen that the difference in adsorption energy is smaller than 0.1 eV for 300 eV and 400 eV cutoff cases. This shows that using cutoff 300 eV gives results accurate enough to be used in analyzing the system. Sampling of the (1x1) and (2x2) Brillouin zones were achieved by summation over Monkhorst-Pack meshes of dimensions 9x9x1 and 5x5x1, respectively.

Exchange and correlation were included via the use of generalized gradient approximation (GGA) along with the Perdew-Burke-Ernzerhof (PBE) functional. It is known that Ni is a ferromagnetic element and spin polarization has an effect on the energy in DFT calculations. However, since this study involves comparison between the adsorption properties of the surfaces which mainly composed of Ni, it is assumed that the spin polarization effect can be neglected. Thus, the same orbital for alpha and beta spins were used in calculations.

Pulay's density mixing scheme was used for the self-consistent field (SCF) electronic minimization. A smearing range of 0.1 eV was applied at the Fermi level and number of additional bands to be included in the electronic minimization was 20 percent of the number of occupied bands. The energy was corrected by extrapolation to zero temperature. The lattice constant of the Ni unit cell is 3.524 Å.

### 3.2. Building and Optimizing Ni Crystal

The unit cell is imported from the pure metal structures of CASTEP (File name: Ni.msi). The ball-and-stick model of the unit cell is given in Figure 3.1.

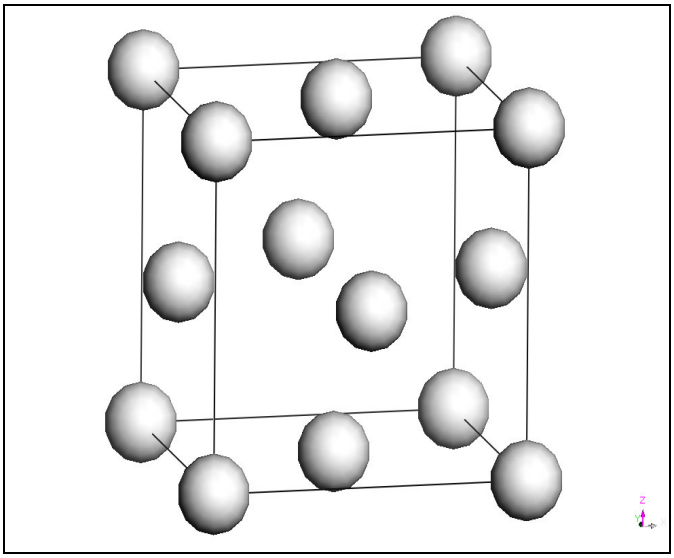

Figure 3.1. The Ni crystal

### 3.3. Building and Optimizing the Ni (111) Surface

There were two steps in building the Ni (111) surface. At first the surface was cleaved according to the geometry; then a vacuum slab was created containing the cleaved surface. To cleave the surface as the first step, the Miller indices of the aimed surface were entered to the specific dialog box "Cleave Surface". The "Depth" of the slab is the desired number of atomic layers of the structure. In this study, number of layers was five, since this provides sufficiently accurate data within a reasonable computational time. Figure 3.2 below shows the structure of cleaved surface of Ni (111).

In order to create a vacuum slab, the thickness of the vacuum layer was determined as a starting point. There is an optimum value of vacuum thickness which decreases both the computational time and the interaction with neighboring slabs. It was found in previous

studies that, selecting 12 Å as the vacuum thickness is an optimal choice in this respect. Figure 3.3 shows the vacuum slab.

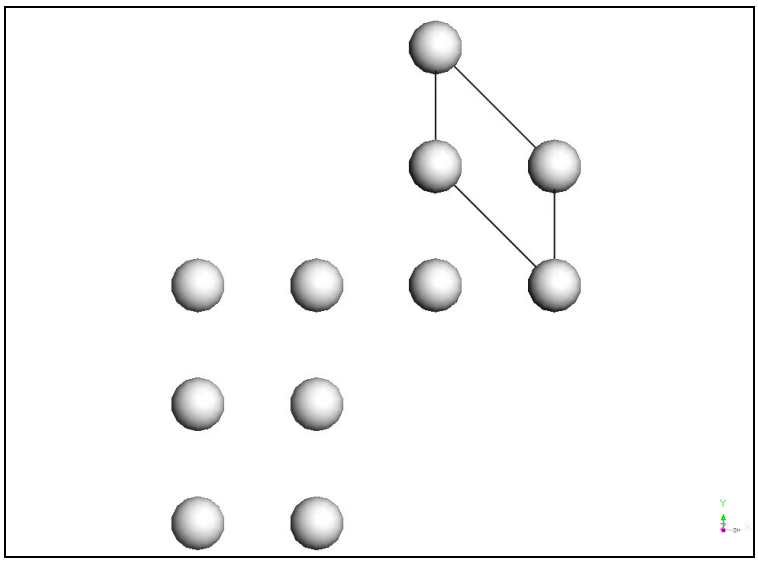

Figure 3.2. The cleaved Ni (111) crystal

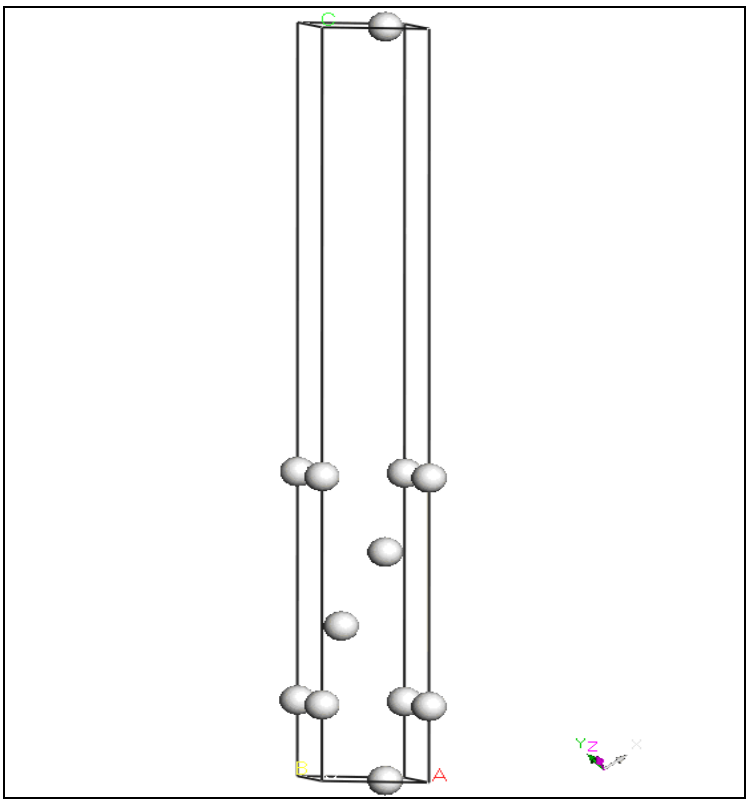


Figure 3.3. The (1 x 1) vacuum slab for the Ni (111) surface

Then, three layers from bottom were selected and the positions of the atoms belong to those layers were frozen; the positions of those atoms were kept fixed during the calculations. Topmost two layers were relaxed and then the slab is energetically and geometrically optimized. After the optimization, five-layers Ni was converted to "Supercell" (2x2) to be used in adsorption studies. In Figure 3.4, a vacuum slab ready for adsorption is seen in "Original, CPK" representation.

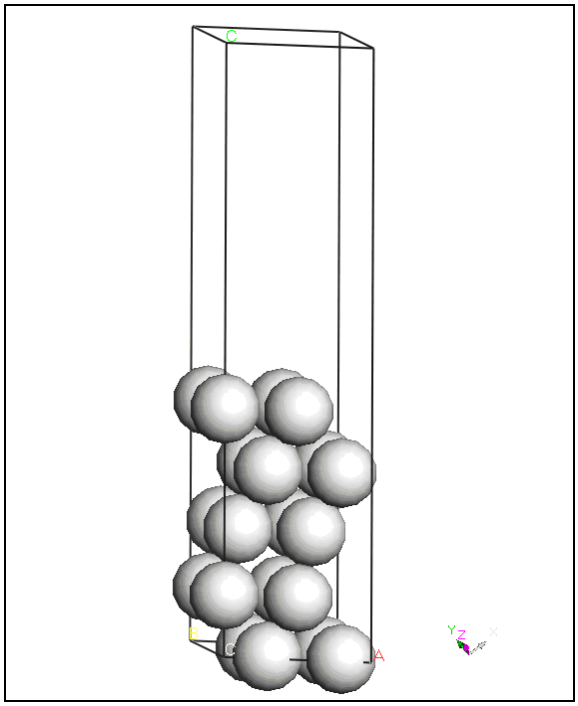


Figure 3.4. Ni supercell

### 3.4. Building the Pt-Ni Surfaces and Layers

After Ni surface was built, the Ni atoms were substituted by Pt atoms either as point defects, or as layers, depending on the aimed surface composition. The Ni atoms to be substituted were selected, and with the "Modify Element" tool in CASTEP, the selected Ni atoms were "converted" to Pt atoms. Resultantly, the Pt-Ni surfaces were obtained. As an example, the surface having "4 bottom layers Ni and topmost Pt layer" is shown as five-layer-vacuum slab in Figure 3.5.

### 3.5. Determination of the Active Sites for Oxygen and $CH_4$ Adsorption

The adsorption sites for O were investigated from previous literature at first. The most known site for O adsorption is fcc site. Though, to check the validity of this data, hcp, bridge and atop sites were also tried in this study and stability of O adsorption on these sites were compared with that on fcc site without changing the other parameters. O adsorption on bridge site was found unstable; O on this site diffused to the neighboring fcc site. The adsorption energies on atop, hcp and fcc sites were calculated as -3.07, -5.07 and -5.17 eV, respectively. The most stable adsorption site in this respect is the fcc site. The difference between the adsorption energies of the fcc and hcp site was calculated as 0.10 eV. This is in accordance with the value reported in the literature as 0.12 eV [28]

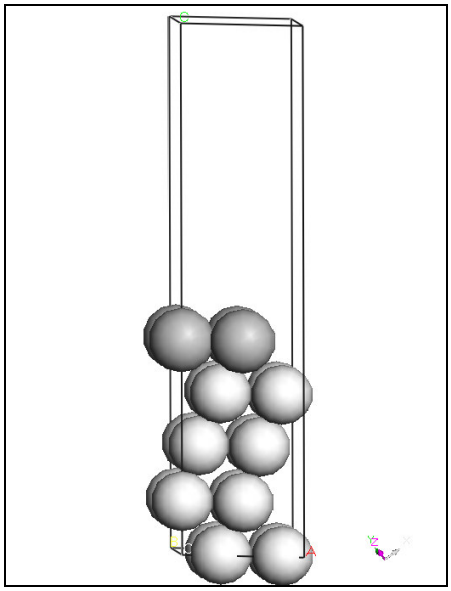

Figure 3.5. 'Ni 4 layers + Pt 1 layer' supercell (○:Ni, ●: Pt)

Top views of Figures 3.5 and 3.6 are shown in Figures 3.7 and 3.8, respectively, as examples. The figures containing the remaining structures with different Pt-Ni surface ratios are given in Appendix B.

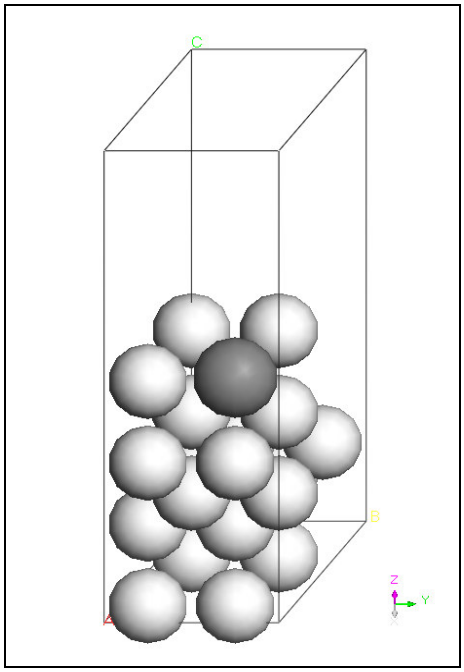


Figure 3.6. 'Ni 5 layers containing 25 per cent Pt at 1st (topmost) layer' supercell (○:Ni, ●: Pt)

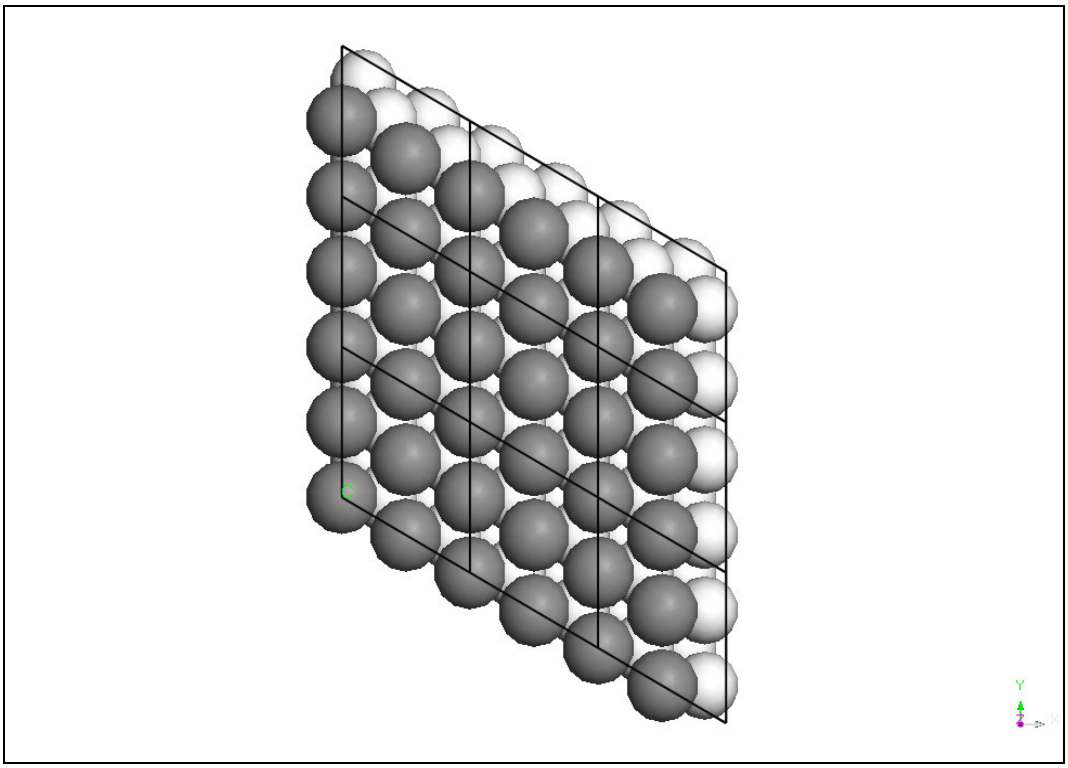


Figure 3.7. Top view of 'Ni 4 layers + Pt 1 layer' (○:Ni, ●: Pt)

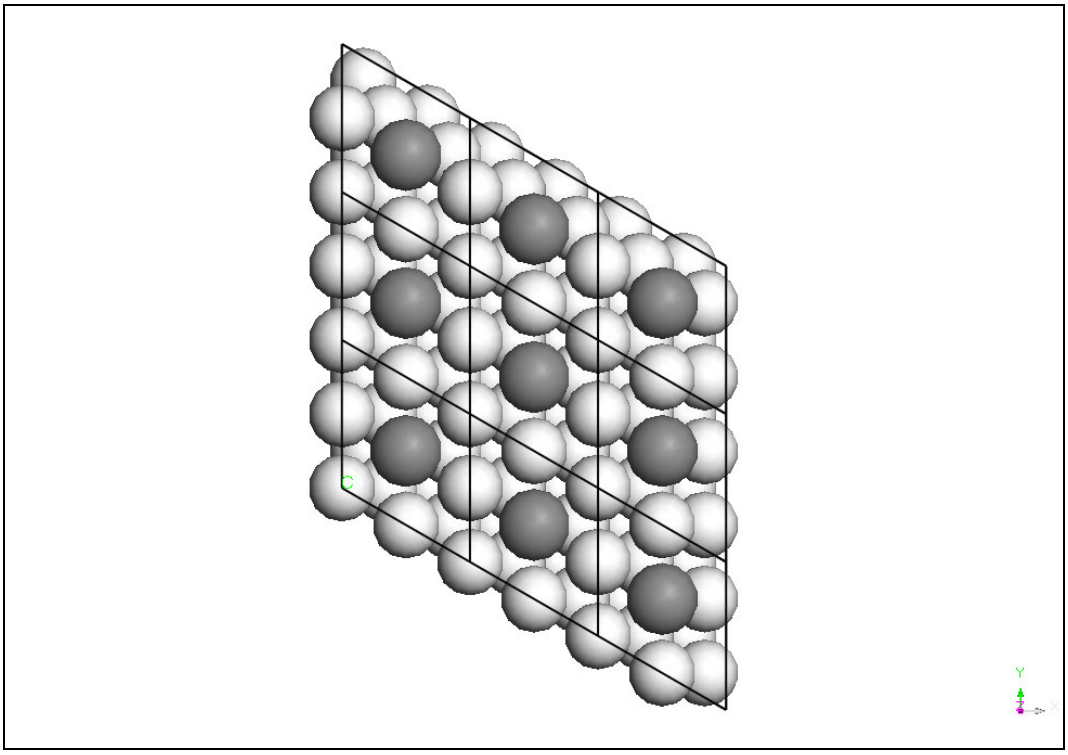

Figure 3.8. Top view of 'Ni 5 layers containing 25 per cent Pt at 1st layer' (○:Ni, ●: Pt)

The possible oxygen adsorption sites on Ni-based surfaces were given in Figure 3.9.

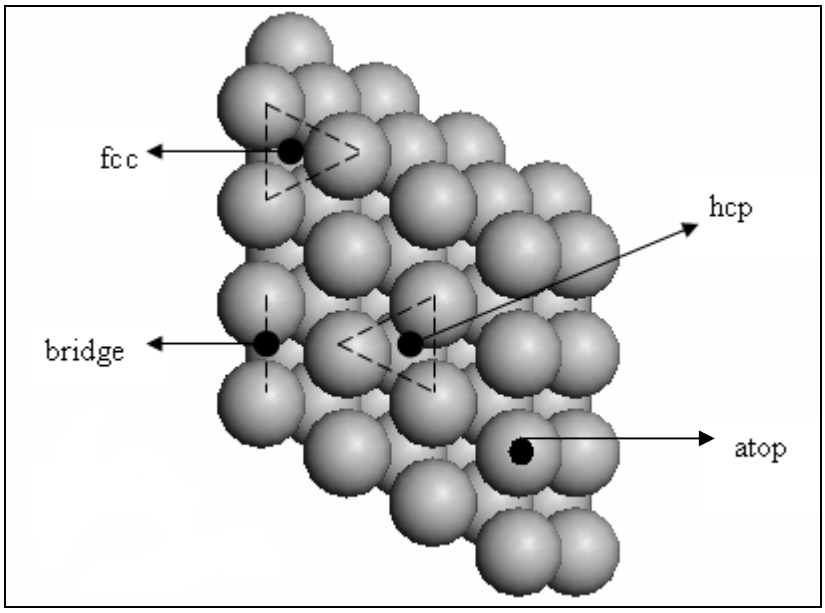


Figure 3.9. Possible Adsorption Sites for Oxygen on Ni-Based Surface

The possible adsorption sites for $CH_4$ were chosen from the literature [26] and are shown in Figure 3.10 below. The $CH_4$ adsorption was considered dissociative; thus, $CH_3$-

was adsorbed on a three fold site; site A and H was adsorbed on the three fold site in the closed-neighborhood, site B.

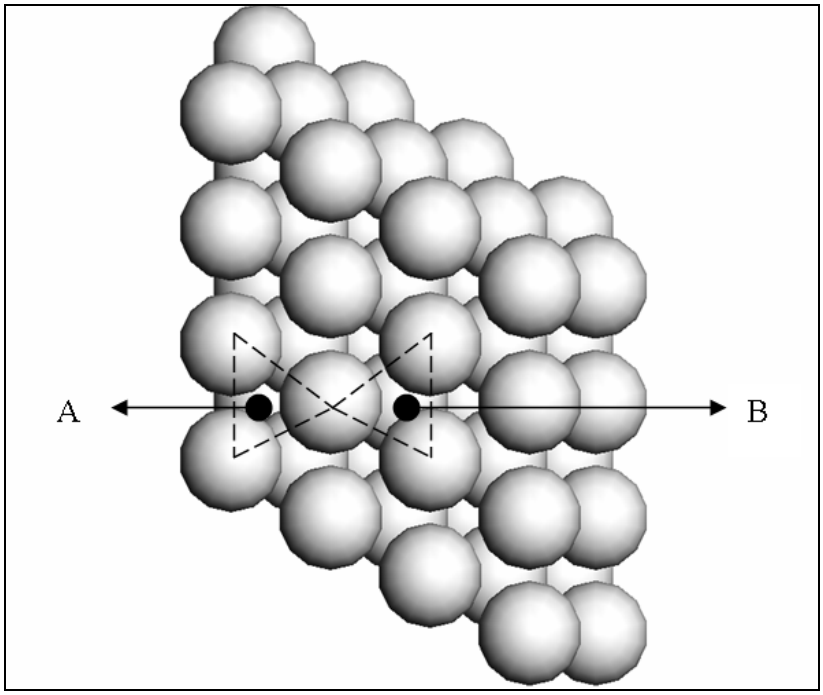


Figure 3.10. Adsorption Site for Methane

### 3.6. Optimization of the Adsorption System

Considering the fact that clean surface energies have a key role in determination of adsorption energies, especially for bimetallic surfaces, the surfaces must be optimized and their energy must be calculated first. In this study, the calculations were performed using the formulas that were previously used by Cabeza et al. [27]. The surface energy σ was expressed as energy per surface atom or per unit surface area:

$$\sigma = \frac{\left(E^{slab} - NE^{bulk}\right)}{2A} \tag{3.1}$$

In the formula; A is the area of the surface unit cell of the slab, $E_{slab}$ is the total energy per unit cell of the five-layer slab, $E_{bulk}$ is the total energy per unit cell of the bulk crystal and N is the number of atoms in the supercell. The factor 2 indicates the presence of

two surfaces in the slab. For bimetallic systems the surface energy ($\sigma_{bim}$) is calculated as follows:

$$\sigma_{bim} = \frac{\left(E^{slab} - N_{subs}^{bulk} E_{subs}^{bulk} - N_{\sup}^{bulk} E_{\sup}^{bulk}\right)}{2A} \tag{3.2}$$

In the formula, $E_{slab}$ is the total energy per unit cell of the bimetallic slab, $N_{subs}^{bulk}$ and $N_{\sup}^{bulk}$ are the numbers of substrate and surface atoms in the slab, respectively, and $E_{subs}^{bulk}$ and $E_{\sup}^{bulk}$ are the energies of a substrate and surface atom in the respective fcc bulk crystals. [27]

To calculate the energy of adsorption system ($E_A$), the following basic formula was used,

$$E_A = E_{(surface+adsorbate)} - E_{(clean\cdot surface)} \tag{3.3}$$

The calculated energies can be seen in the related tables in Chapter 4.

### 3.7. Plotting the LDOS Charts

Aiming to understand the electronic nature of the adsorption systems at atomic scale, the local density of states (LDOS) profiles were utilized.

In an optimized system, the atom(s) of interest was selected and, the LDOS profiles of those atoms were produced in the simulations. In order to have LDOS of selected atoms, "Calculation/Analysis" tool of CASTEP, "Analysis" and "Density of States" part was chosen. Then by clicking the "View", the LDOS profile was obtained.

In order to compare the LDOS profiles of the same atom for different cases, data were copied to excel, the graphs were created on the same scale, and that the results were compared.

### 3.8. Calculation of Surface Stress of Clean Surfaces

In order to calculate the stress of the clean surfaces, stress tensor data was extracted from the output file of CASTEP. Stress tensor has components in x, y and z direction. Since the atoms can expand in z direction through the vacuum, only the data in x and y direction were taken into consideration for this study where stress is defined as the average value of the two diagonal elements for each surface;

$$Stress = \frac{(x_{11} + y_{22})}{2} \tag{3.4}$$

In the formula $x_{11}$ and $y_{22}$ are the two of three diagonal elements of the stress tensor.

For applying the equation 3.4 for Ni 5 layers surface as an example, "Stress Tensor in Cartesian Coordinates (GPa)" data needed are gathered from CASTEP output as shown below:

Table 3.1. Surface Tensor in Cartesian Coordinates (GPa)

| | x | y | z |
|---|---|---|---|
| x | 2.38008 | 0.00019 | 0.00007 |
| y | 0.00019 | 2.37986 | -0.00128 |
| z | 0.00074 | -0.00012 | -3.18020 |

Then surface stress for 5 Ni layers surface can be calculated as;

$$Stress = \frac{(2.38008 + 2.37986)}{2} \approx 2.38 \quad GPa$$

# 4. RESULTS AND DISCUSSION

In this theoretical study, the interaction between Pt-Ni bimetallic surfaces and main OSR reactants, oxygen and methane, was investigated. Since the energy of the clean surface has a pronounced effect on adsorption strength and energy of adsorption, clean Pt-Ni surfaces, having different Pt contents, were generated and the effect of Pt insertion on surface energy properties was also analyzed, prior to the studies on adsorption properties of Pt-Ni surface. Pt amount in the upper layer(s) of the flat Ni surfaces were changed in a parametric fashion both for studies on properties of clean surfaces and for studies on O-Pt/Ni and $CH_4$-Pt/Ni.

## 4.1. Properties of Clean Pt-Ni Surface

Considering the fact that surface energy is a measure of the stability of the surface and it decreases with the enhanced surface stability, the surface energies of the clean Pt-Ni surfaces were calculated and compared first. Additionally, interlayer spacing i.e. the distance between the first and the second layer of the vacuum slab, which is an important property showing the effect of Pt presence, was calculated. The relation between interlayer spacing and clean surface energy are related and is discussed.

### 4.1.1. Pure Monometallic Surfaces

There were two different monometallic surfaces in this study; Ni 5 layers and Pt 5 layers. The data of the pure monometallic surfaces were used as the reference bases in analyzing the properties of bimetallic Pt-Ni surfaces

### 4.1.2. Ni-Pt Surface Alloys

The surface tension of Pt (111) surface is smaller than that of Ni (111) surface. Based on this finding and considering the fact that Pt atom size is larger than that of Ni atoms, it is not surprising that addition of Pt in place of Ni atoms on Ni (111) surface increases the

stability of the surface, which is indicated by the decrease in surface tension. It was reported in the literature that; interlayer spacing between the first and second layers is inversely proportional to the surface tensile stress. [29] In this study, addition of Pt to Ni metal decreases the tensile stress on the catalyst surface, which manifests itself as an increase in the interlayer spacing. Resultantly, the surface energy increases with increasing Pt concentration and interlayer spacing. The relation between interlayer spacing, surface energy and surface stress is given in Figure 4.1. The surface energy and interlayer spacing values for various bimetallic surfaces are given in Table 4.1. Figure 4.2 shows how surface energy changes with the interlayer spacing between the first and second layers of Pt/Ni systems studied. Note that (i) the reference Ni system has 5 Ni layers, (ii) in order to generate Pt/Ni surfaces that only have Pt atoms at the topmost layer with surface concentrations in 25-75 per cent range, the Ni atoms present on the upmost Ni surface are changed with Pt atoms, and (iii) for generating a Pt layer on top of 4 layers of Ni, the Ni atoms in the topmost layer of reference Ni surface are fully replaced by Pt atoms.

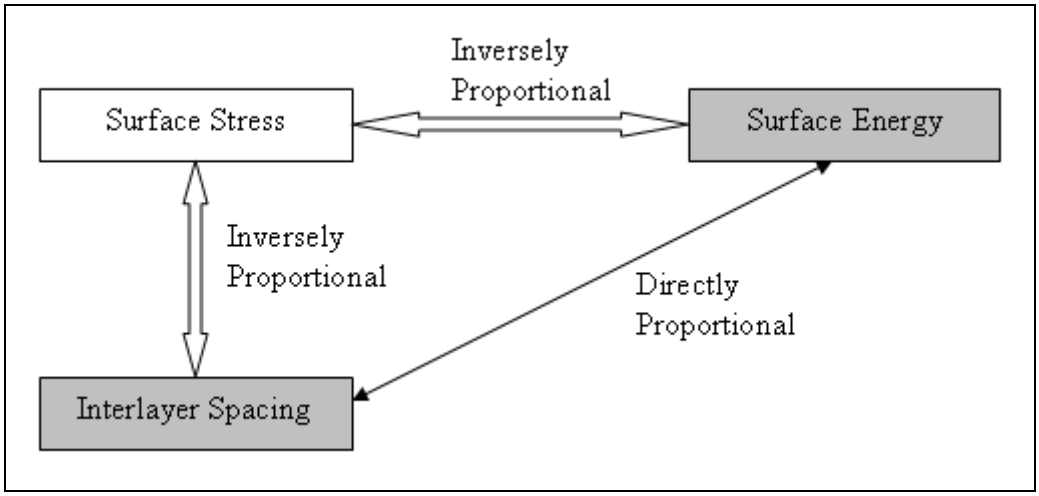


Figure 4.1. Schematic Representation of the relationship between Surface Energy and Interlayer Spacing of the 1st and 2nd layers of the slab

Table 4.1. Surface Energy vs. Interlayer Spacing between the 1st and 2nd layers of Pt-Ni systems

| Clean Surface | Surface Energy ($J/m^2$) | Interlayer Spacing (Å) |
|---|---|---|
| 'Ni 5 layers containing 25 per cent Pt at 1st layer' | 1.61 | 2.09 |
| 'Ni 5 layers containing 50 per cent Pt at 1st layer' | 1.63 | 2.15 |
| 'Ni 5 layers containing 75 per cent Pt at 1st layer' | 1.83 | 2.25 |
| 'Ni 4 layers + Pt 1 layer' | 2.37 | 2.34 |

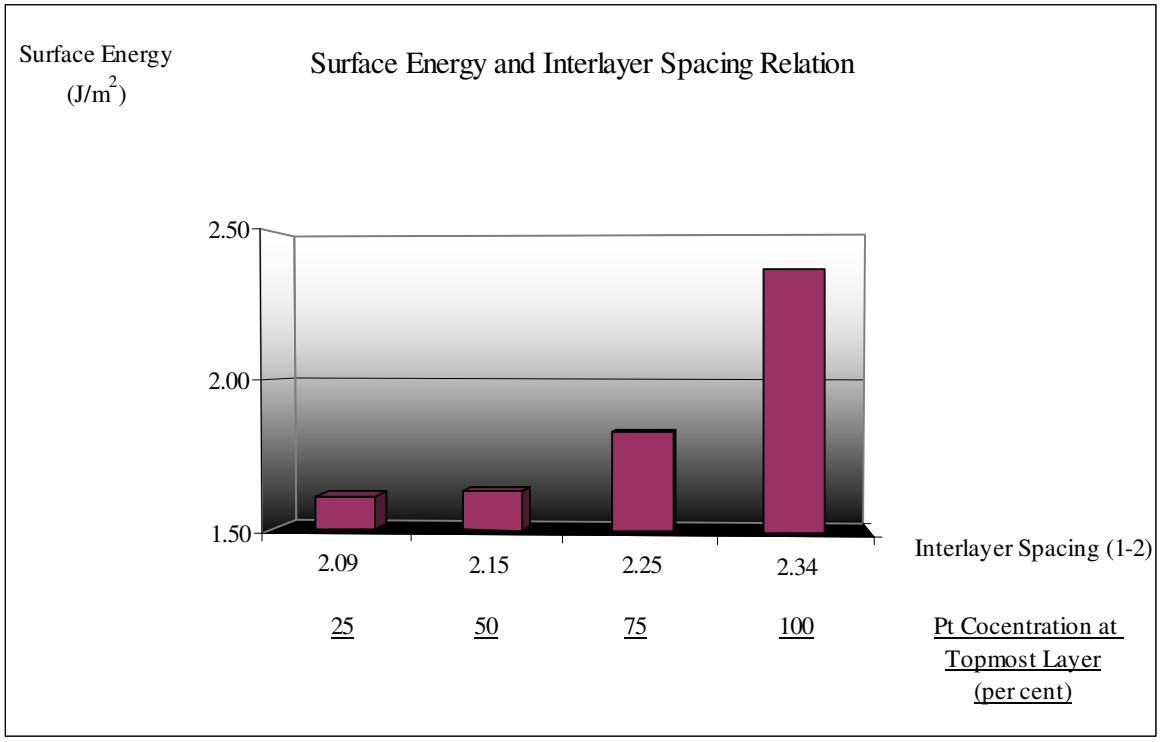


Figure 4.2. Change of Surface Energy with Interlayer Spacing between the 1st and 2nd Layers of Pt-Ni systems

The first "clean surface energy" calculation was performed with pure Ni five-layer-slab i.e. 'Ni 5 layers'. Then, Pt content at the topmost layer was increased in parametric fashion. Equations 3.1 and 3.2 were used in energy calculations. The changes in energy with Pt percent at topmost layer are shown in Table 4.2 and in Figure 4.3 below.

Table 4.2. Surface Energy vs. Pt concentration for clean Pt-Ni systems

| Clean Surface | Surface Energy ($J/m^2$) | Pt Content (per cent) |
|---|---|---|
| 'Ni 5 layers' | 1.79 | 0 |
| 'Ni 5 layers containing 25 per cent Pt at $1^{st}$ layer' | 1.61 | 25 |
| 'Ni 5 layers containing 50 per cent Pt at $1^{st}$ layer' | 1.63 | 50 |
| 'Ni 5 layers containing 75 per cent Pt at $1^{st}$ layer' | 1.83 | 75 |
| 'Ni 4 layers + Pt 1 layer' | 2.37 | 100 |
| 'Ni 3layers + Pt 2 layers' | 3.79 | 100 |
| 'Ni 5 layers containing 25 per cent Pt at $2^{nd}$ layer' | 1.86 | 25 |

It is calculated that the surface energy of Ni (111) is decreased from 1.79 $J/m^2$ to 1.61 $J/m^2$ when Pt concentration at the topmost layer is increased from 0 to 25 per cent. Addition of Pt atoms to increase the surface concentration to 50 per cent, leads to a small increase in the surface energy to 1.63 $J/m^2$. Further increase in the Pt concentration on the topmost layer decreases the stability of the surface. The surface energy continues to increase and becomes 1.83 $J/m^2$ at 75 per cent Pt concentration at the topmost layer, and the surface energy becomes 2.37 $J/m^2$ when the topmost layer is fully covered with Pt atoms. Addition of more Pt i.e. increasing the number of Pt layers on top of Ni layers to two, on the other hand, increases the surface energy to 3.79 $J/m^2$, i.e., decreases the stability further. As shown in Figure 4.3 below, surface energy is at minimum when Pt concentration at the topmost layer is 25 per cent, which means this is the most stable structure.

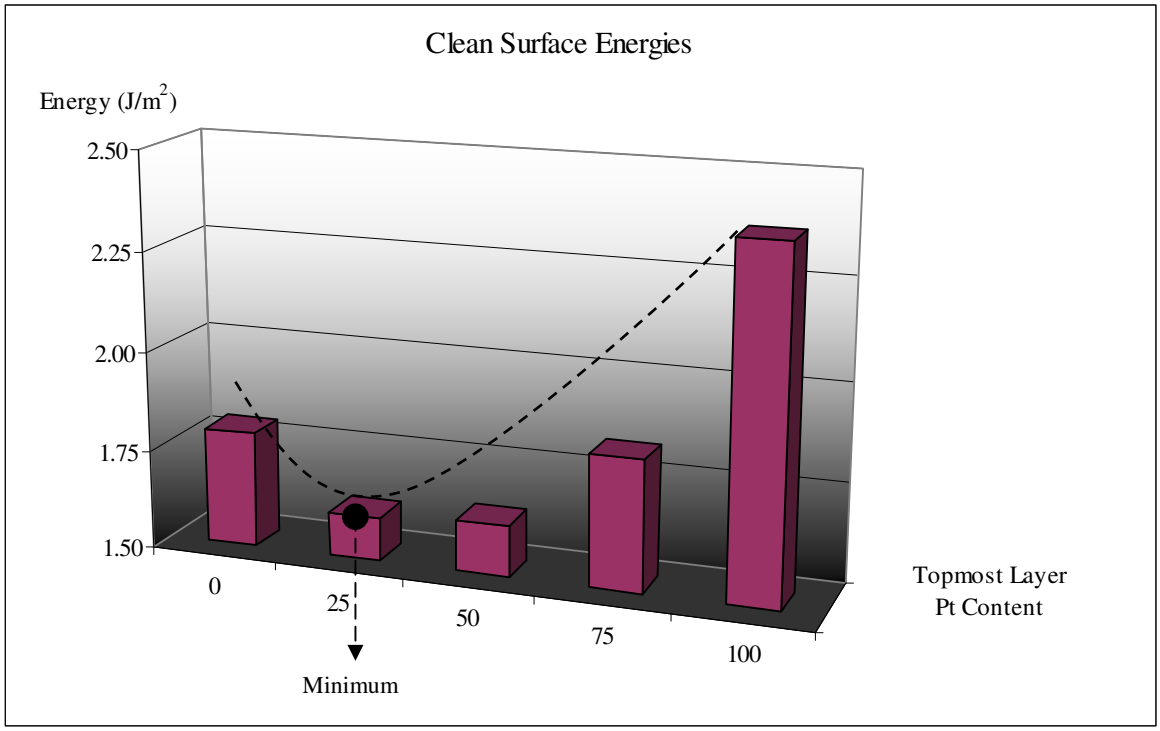


Figure 4.3. Change of Surface Energy with Pt Concentration at Topmost Layer of Pt/Ni system

Additionally, surface segregation of Pt from topmost layer ('Ni 5 layers') to the second layer, decreases the stability of the surface. The energy of segregation on Pt atom at a surface concentration of 25 per cent from topmost layer to the second layer ('Ni 5 layers containing 25 per cent Pt at 2$^{nd}$ layer'), i.e. the surface has 5 Ni layers for which the second layer from the top has 25 per cent Pt, causes 0.25 eV energy increase, meaning a decrease in stability (Table 4.2). This means unlike Pt addition on the topmost layer, Pt insertion in bulk Ni is not favored energetically.

The changes in the surface energy depend on the surface stress. On pure Ni (111), there is an effective tensile stress on the surface due to undercoordination of surface atoms. CASTEP measured it as 2.38 (positive value means tensile stress is effective). 25 per cent Pt substitution to Ni surface decreases tensile stress to 0.90 GPa. This decrease in stress makes the 'Ni 5 layers containing 25 per cent Pt at 1$^{st}$ layer' surface more stable than pure Ni structure ('Ni 5 layers'). Addition of more Pt to the surface, i.e. 'Ni 5 layers containing 50 per cent Pt at 1$^{st}$ layer', this time causes compression between the surface atoms. The value of the surface stress becomes negative confirming compressive stress is effective

instead of tensile stress for those higher Pt concentrations at the topmost layer. In general, the case for which surface stress is closest to zero (either tensile or compressive stress) gives the most stable structure, which is 'Ni 5 layers containing 25 per cent Pt at 1st layer' in this case. (Table 4.3 and Figure 4.4)

Table 4.3. Pt Concentration and Stress data for Pt-Ni systems

| Surface Name | Pt Content (per cent) | Stress (GPa) |
|---|---|---|
| 'Ni 5 layers' | 0 | 2.38 |
| 'Ni 5 layers containing 25 per cent Pt at 1st layer' | 25 | 0.90 |
| 'Ni 5 layers containing 50 per cent Pt at 1st layer' | 50 | -1.85 |
| 'Ni 5 layers containing 75 per cent Pt at 1st layer' | 75 | -5.00 |
| 'Ni 4 layers + Pt 1 layer' | 100 | -11.54 |

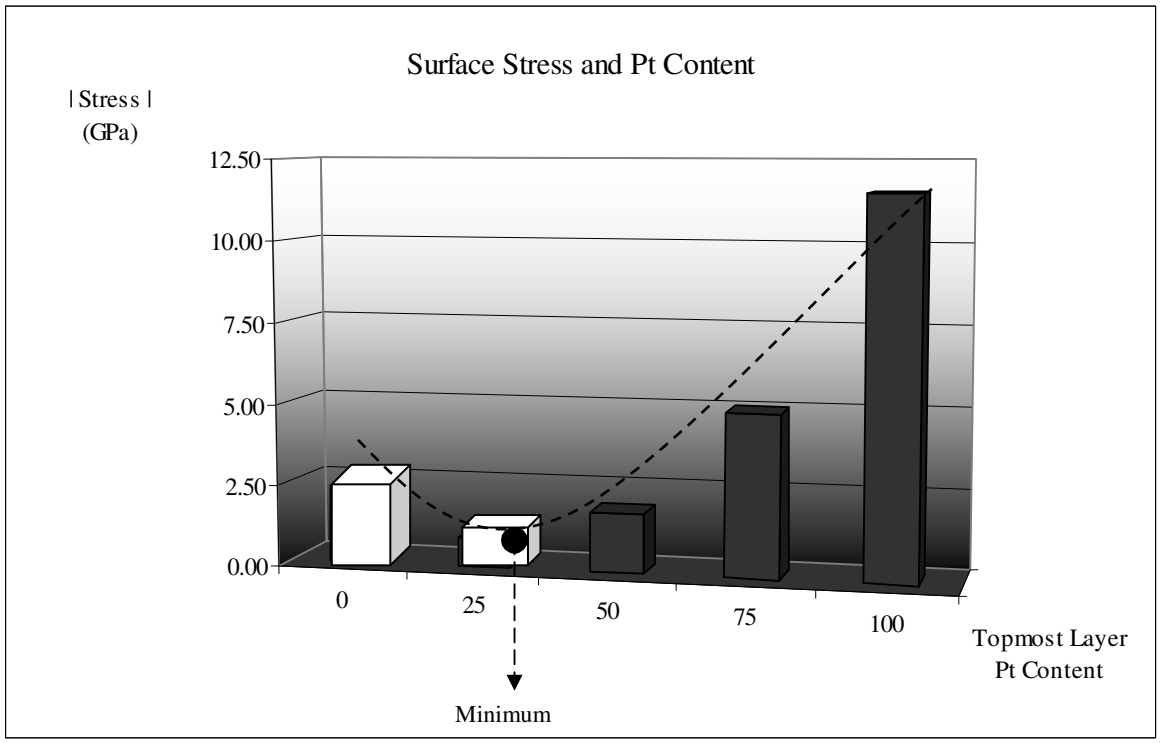


Figure 4.4. Change of Surface Stress with Pt Concentration at Topmost Layer of Ni 5 Layers (□: Tensile Stress, ■: Compressive Stress)

It is interesting to note that the case for which surface tensile stress is at its minimum, i.e. surface Pt concentration at topmost layer is 25 per cent, the surface structure is at its

maximum stability, i.e. the surface energy is at minimum. The analysis indicate that that the stability of a surface alloy is strongly affected by surface stress and in the case of Pt-Ni bimetallic system, the lowest stress value calculated for 'Ni 5 layers containing 25 per cent Pt at 1$^{st}$ layer' surface alloy makes its formation favorable.

Considering the fact that Pt substitution has a direct effect on the electronic properties of the atoms, local density of states (LDOS) of the corresponding surface atoms were investigated. As the amount of added Pt to the top layer increases (shown on Figure 4.5), the LDOS peak intensity of Ni atom on the topmost surface decreases between -2 and -1 eV energy range.

In Figure 4.5, the decrease in Ni LDOS curves resulted from electron transfer from Ni atoms to Pt atoms on the surface. The total area under LDOS curves is a direct measure of the amount of charge (i.e. electron density) at the valence-band of metal atoms. Although, it is not enough to analyze the magnitude of total change transfer between Ni and Pt fully, it is adequate to conclude that, as Pt concentration on the surface increased, charge depletion on Ni atoms in the energy levels which involve strongly in band formation ca. -2 eV, increased. A comparison of LDOS profiles for Pt substitutions into first or second layers of Ni 5 layers show that; LDOS profiles are very similar, meaning the electronic structures are similar (Figure 4.6). On the other hand, when Pt atom was located in the second layer instead of topmost layer, Pt atom was stuck more than it was in first layer. It is important to note that not the electronic structure, but the stuck of Pt atom in Ni lattice caused 0.25 J/m$^2$ energy difference (Table 4.2, second and last data).

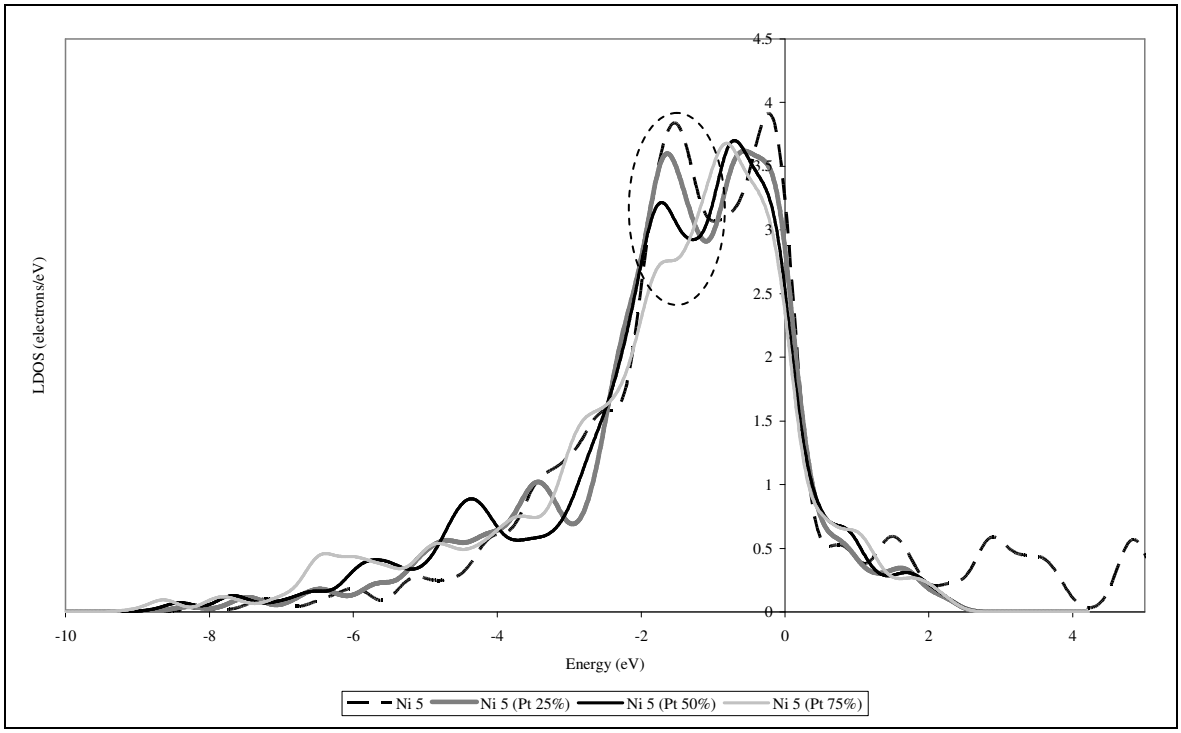


Figure 4.5. Clean Surface LDOS Profiles of Ni atom of Ni and Pt/Ni surfaces with Different Pt Contents at the Topmost Layer

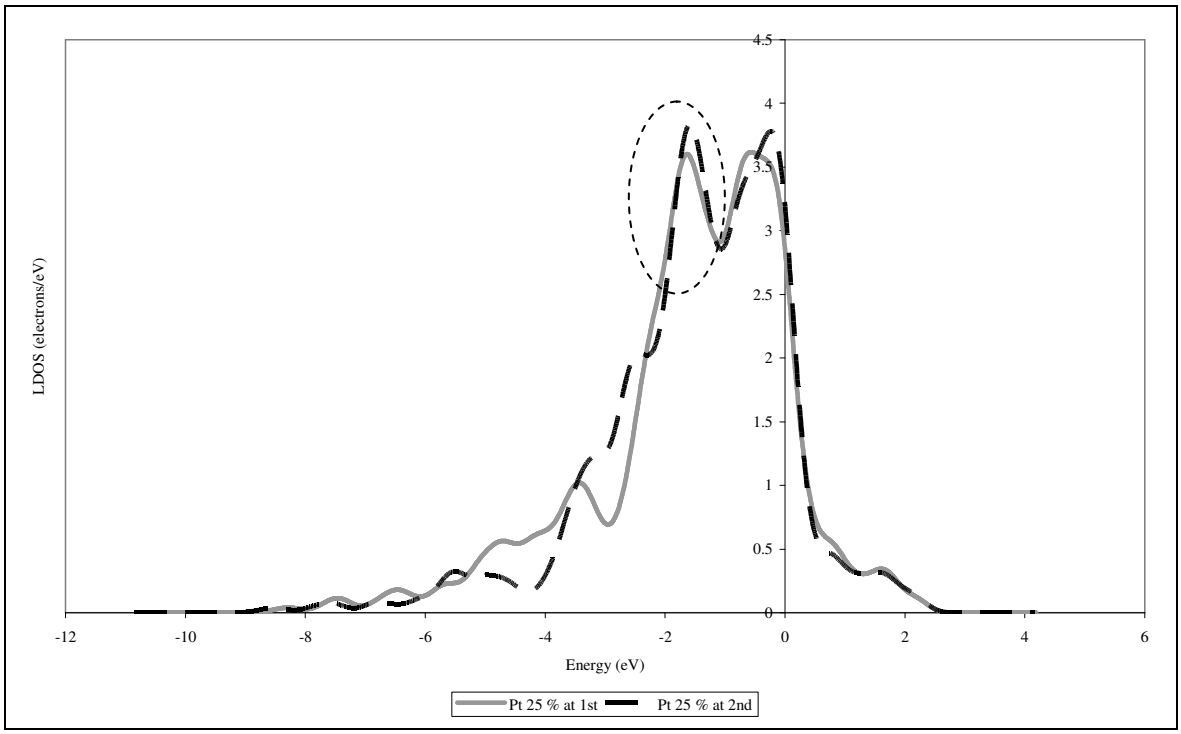


Figure 4.6. Clean Surface LDOS Profiles of Ni 5 Layers with Pt content 25 per cent at 1st and at 2nd Layer (Nickel Atom)

## 4.2. Oxygen Adsorption

### 4.2.1. Adsorption on Ni-Pt Surface Alloys

The most stable O adsorption site on both Ni (111) and Pt (111) surface is fcc site. The presence of Pt decreases the strength of O adsorption on Ni an Ni-Pt sites. The decreasing adsorption strength of oxygen is led by the combined effects of the following changes in the electronic and geometric (ensemble) structure of the surfaces, these are; (i) changing concentrations of Pt has influence on the total surface energy and the stability of the clean surface, which has a direct effect on the adsorption energy of oxygen, (ii) Pt acts as a diluent of the Ni matrix and with the increase in Pt concentration, possible fcc type adsorption sites starts having Pt atoms, which directly interacts with the adsorbed oxygen, (iii) presence of Pt changes the electronic properties, i.e. LDOS profiles, of both the Ni and Pt atoms present at the fcc type adsorption sites through electronic interactions.

In order to analyze the reason why adsorption becomes weaker when there is Pt substitution, the nature of the chemical bond between O and metal had to be checked. The bond between O and metal constitutes of an ionic and a covalent part. [30]

The analysis of the adsorption properties of the sites through using work function is a powerful tool, especially for bimetallic surfaces and sites. Ionic interaction is essentially an electrostatic interaction and based on the charge transfer from metal to oxygen. When Ni was substituted by Pt in Pt-Ni surface alloys, the work function increased proportionally with increasing Pt concentration. This increase in work function is related to the electronic reconstruction of surface metal atoms which results from electron transfer from Ni to Pt. This increase in work function decreases electron transfer from metal to O and resultantly weakened the ionic interaction of the metal. The work function is the minimum energy, measured in electron volts, which is needed to remove an electron from a solid to a point immediately outside the solid surface. On the surface of the catalysts, as Pt content at the topmost layer increases, work function increases. The changes in the work function of the fcc sites on Pt-Ni surface, for $fcc_{Ni3}$ on 'Ni 5 layers' and 'Ni 5 layers containing 25 per cent Pt at 1$^{st}$ layer' surface, and for $fcc_{Ni2Pt1}$ on 'Ni 5 layers containing 50 per cent Pt at 1$^{st}$ layer' surfaces, are given in Table 4.4 and Figures A.1-3 in Appendix A. Increase in work

function leads to a decrease in the tendency of metal atoms to supply electrons to the adsorbates. The approach that, as the stability increases, since oxygen cannot gain electrons due to the increase in work function, the adsorption of oxygen becomes weaker, will be tried to be confirmed in the following section through on the basis of the calculated O adsorption strengths on those sites.

Table 4.4. Change of Work function with increasing Pt content on Pt-Ni systems

| Surface Name | Work function (eV) | Pt Content (per cent) |
|---|---|---|
| 'Ni 5 layers' | 5.23 | 25 |
| 'Ni 5 layers containing 25 per cent Pt at 1$^{st}$ layer' | 5.32 | 50 |
| 'Ni 5 layers containing 50 per cent Pt at 1$^{st}$ layer' | 5.37 | 75 |

In order to analyze the effect of Pt on the adsorption properties of the fcc sites of Pt-Ni surfaces; the adsorption properties of all possible adsorption sites with changing number of Pt-O bonds were compared for each Pt surface concentrations. The results of the calculations are given in Table 4.5 and Figure 4.6) At a total Pt surface concentration of 25 per cent, there were two possible fcc adsorption sites on the surface; in 'Ni 5 layers containing 25 per cent Pt at 1$^{st}$ layer' 'F.25-1' - O/$fcc_{Ni2Pt1}$, there is one platinum atom at one of the three legs of oxygen atom and in 'Ni 5 layers containing 25 per cent Pt at 1$^{st}$ layer' - O/$fcc_{Ni3}$ there is not any platinum atom at the legs of adsorbed oxygen atom. Adsorption on site $fcc_{Ni3}$ is stronger by 0.38 eV than that on $fcc_{Ni2Pt1}$. The clean surface structure was the same for both cases, thus, the only difference causing the changes in the adsorption strength was the increased number of O-Ni bonds. Similarly, at a total Pt surface concentration of 50 per cent, there were two possible fcc adsorption sites on the surface 'Ni 5 layers containing 50 per cent Pt at 1$^{st}$ layer' - O/$fcc_{Ni2Pt}$ (containing one platinum at one leg), and "Ni 5 layers containing 50 per cent Pt at 1$^{st}$ layer' - O/$fcc_{Ni1Pt2}$ (containing two platinum at both legs). Adsorption on site $fcc_{Ni2Pt}$ is stronger by 0.41 eV than on $fcc_{NiPt2}$, which resulted from the increased number of Ni-O bonds. The magnitude of the adsorption strength differences led by the changes in bonding chemistry seems to be similar at all surface Pt concentrations tested in this study and equals to approximately 0.4 eV per Ni-O bond. Thus as a general trend, with the increase in surface Pt concentration,

the Ni atoms present at the adsorption site is/are replaced by the Pt atoms and, as a consequence, stronger Ni-O interaction at fcc sites are replaced by relatively weak Pt-O interactions, which results in weaker adsorption.

Keeping the chemical adsorption structure same, i.e. using fixed number of Pt-O and Ni-O bonds, the relation between the adsorption strength of a site and the stability of the clean surface can be analyzed on the basis of total surface energy. The difference between the adsorption energy of $fcc_{Ni3}$ site is 0.44 eV on surface of Ni 5 layers, i.e. with a total surface Pt concentration 0 and 25 per cent. The presence of a Pt atom in the neighborhood decreases the stability of the $fcc_{Ni3}$ site, although Pt itself is not involved in the bonding itself. On the other hand, a similar reasoning is not correct for a Pt neighbor present in the subsurface; on the surface 'Ni 5 layers containing 25 per cent Pt at 2$^{nd}$ layer' formed by substituting a Pt atom in place of Ni at the second layer making a Pt concentration of 25 per cent for subsurface, the adsorption on $fcc_{Ni3}$ site is stronger by 0.59 eV, compared with that on surface 'Ni 5 layers containing 25 per cent Pt at 1$^{st}$ layer'. The main reason of these varying adsorption strengths due to the changes in the concentration and position of neighbor atoms is found to be strongly correlated with the stability of the clean surface. The analysis of the differences between the surface energy of the clean surface per cell, it is seen that the difference between the surface energy of 'Ni 5 layers containing 25 per cent Pt at 1$^{st}$ layer' and ‘Ni 5 layers' is -0.53 eV per cell, whereas it is 0.59 eV per cell between surface 'Ni 5 layers containing 25 per cent Pt at 1$^{st}$ layer' and 'Ni 5 layers containing 25 per cent Pt at 2$^{nd}$ layer'. This shows that when the initial surface is stable, adsorption on this surface is weak for the similar sites, whereas when the stability decreases, the strength of adsorption increases.

For adsorption on $fcc_{Ni2Pt}$ site, presence of a Pt neighbor at surface concentration of 50 per cent Pt ('Ni 5 layers containing 50 per cent Pt at 1$^{st}$ layer' - O/$fcc_{Ni2Pt}$) decreases the strength of $fcc_{Ni2Pt}$ site by 0.40 eV (from -4.34 eV to -3.94 eV shown in Table 4.5); compared to the adsorption energy of the same site at the surface concentration of 25per cent Pt ('Ni 5 layers containing 25 per cent Pt at 1$^{st}$ layer' - O/$fcc_{Ni2Pt}$).

Table 4.5. Energy and Bond Length data for clean and O adsorbed Pt-Ni systems

| Surface Name | Clean Surface Energy ($J/m^2$) | Adsorption Energy ($E_A$) (eV) | Bond Lengths (Å) | | |
|---|---|---|---|---|---|
| 'Ni 5 layers'-$fcc_{Ni3}$ | 1.79 | -5.16 | 1.84 | 1.84 | 1.84 |
| 'Ni 5 layers containing 25 per cent Pt at 1st layer'-$fcc_{Ni3}$ | 1.61 | -4.72 | 1.85 | 1.85 | 1.85 |
| 'Ni 5 layers containing 25 per cent Pt at 1st layer'-$fcc_{Ni2Pt}$ | 1.61 | -4.34 | 1.85 | 1.85 | 2.09 |
| 'Ni 5 layers containing 50 per cent Pt at 1st layer'-$fcc_{Ni2Pt}$ | 1.63 | -3.94 | 2.07 | 1.85 | 1.85 |
| 'Ni 5 layers containing 50 per cent Pt at 1st layer'-$fcc_{NiPt2}$ | 1.63 | -3.52 | 2.09 | 2.08 | 1.85 |
| 'Ni 5 layers containing 75 per cent Pt at 1st layer'-$fcc_{NiPt2}$ | 1.83 | -3.29 | 2.02 | 2.21 | 1.85 |
| 'Ni 5 layers containing 75 per cent Pt at 1st layer'-$fcc_{Pt3}$ | 1.83 | -2.72 | 2.11 | 2.11 | 2.10 |
| 'Ni 4 layers + Pt 1 layer'-$fcc_{Pt3}$ | 2.37 | -3.75 | 2.31 | 2.04 | 2.05 |
| 'Ni 3 layers + Pt 2 layers' -$fcc_{Pt3}$ | 3.79 | -6.56 | 2.09 | 1.97 | 3.80 |
| 'Pt 5 layers'-$fcc_{Pt3}$ | 1.59 | -3.85 | 2.08 | 2.07 | 2.07 |

In Figure 4.7, adsorption energy data can be analyzed more clearly. As the concentration at topmost layer of 'Ni 5 layers' surface were increased; and resultantly number of Pt-O bonds increased; the adsorption strength became weaker, among which adsorption on 'Ni 5 layers containing 75 per cent Pt at 1st layer' was the weakest strength for oxygen.

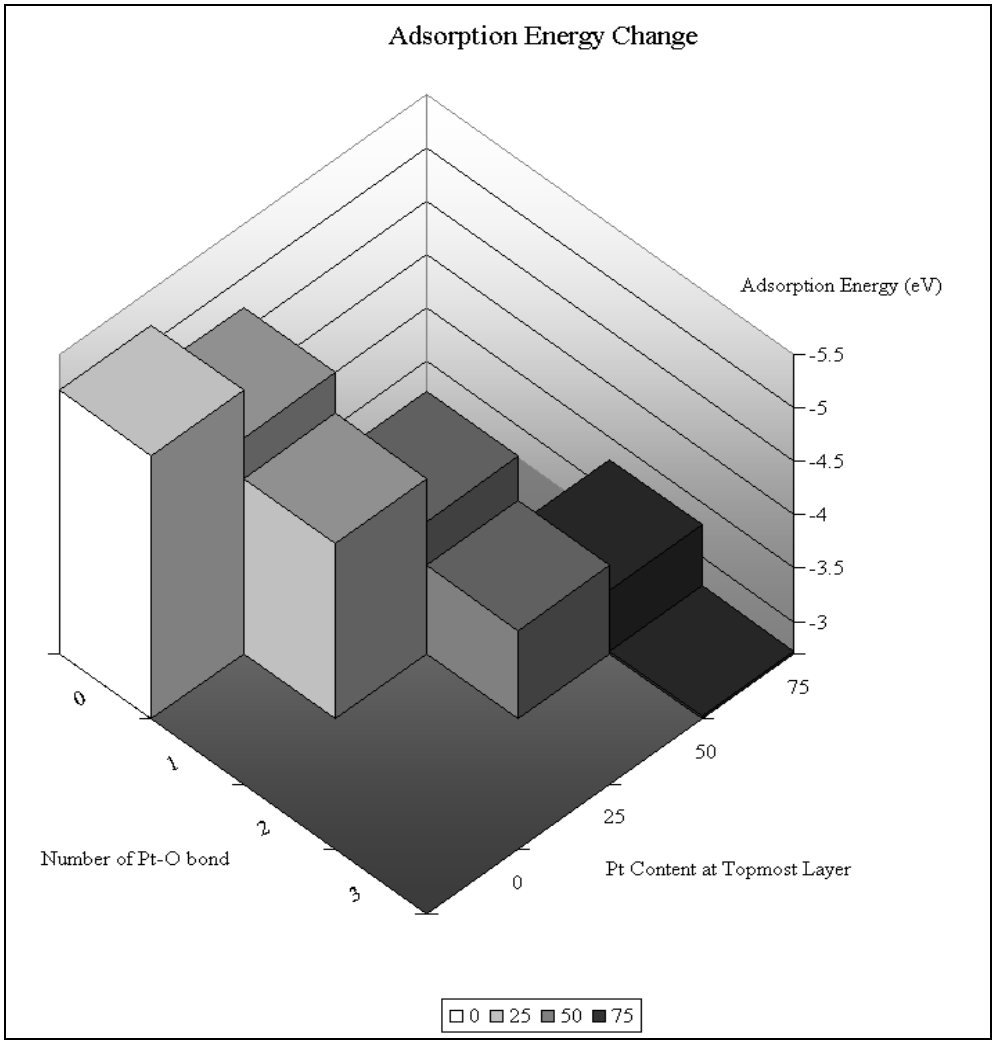


Figure 4.7. Change of Adsorption Energy of Oxygen on Ni 5 layers with Pt Concentration at 1st Layer and with Number of Pt-O Bonds

The electronic interaction between the atoms present at the adsorption site and the adsorbate O can be analyzed through evaluating the LDOS profiles of both the metal atoms involved in adsorption and LDOS that of oxygen. The LDOS profiles of mutual atoms at adsorption sites and LDOS profile of adsorbed O give information on the electronic interaction between O and metal atoms, and how the electronic behavior changes through Pt-Ni interactions for bimetallic surfaces as well. It is shown in Figure 4.8 that the peak intensity in 0-(-5) eV region, decreases for Ni atom upon adsorption. Since oxygen is electronegative, there is electron transfer from nickel atoms to oxygen adsorbed on them. So the difference arises from the nature of bonding. Figure 4.9 shows the LDOS profiles of Ni for oxygen adsorption on Ni and Pt-Ni surfaces 'Ni 5 layers' and 'Ni 5 layers containing 25 per cent Pt at 1st layer'. As can be seen from the comparison of the LDOS profiles of

one of the Ni atoms present at the O coordinated $fcc_{Ni3}$ sites on 'Ni 5 layers' and 'Ni 5 layers containing 25 per cent Pt at 1st layer' surfaces (Figure 4.9) there is slightly higher electron density at ca. (-2) eV for Ni at 'Ni 5 layers' surface whereas the electron density is significantly lower the same Ni at ca. (-5) eV compared to that on 'Ni 5 layers containing 25 per cent Pt at 1st layer' surface. The differences in Ni LDOS profiles clearly shows the change in electronic behavior of Ni-O interaction led by the electron transfer from Ni atom to the Pt in the neighborhood on 'Ni 5 layers containing 25 per cent Pt at 1st layer' surface. Resultantly, the electron transfer from Ni to O decreased, as indicated by the comparison of adsorbed O on $fcc_{Ni3}$ sites of 'Ni 5 layers' and 'Ni 5 layers containing 25 per cent Pt at 1st layer' surfaces (Figure 4.10) It is clearly seen that, the electron transfer from Ni to O for 'Ni 5 layers' surface is higher. Pt has shared Ni's electrons and less electrons are left for O atom. Figure B.5, which compares LDOS of adsorbed O on $fcc_{Ni3}$ sites of Ni 5 and 'Ni 5 layers' and 'Ni 5 layers containing 25 per cent Pt at 1st layer' surfaces, can be explained similar to the profiles in Figure 4.10.

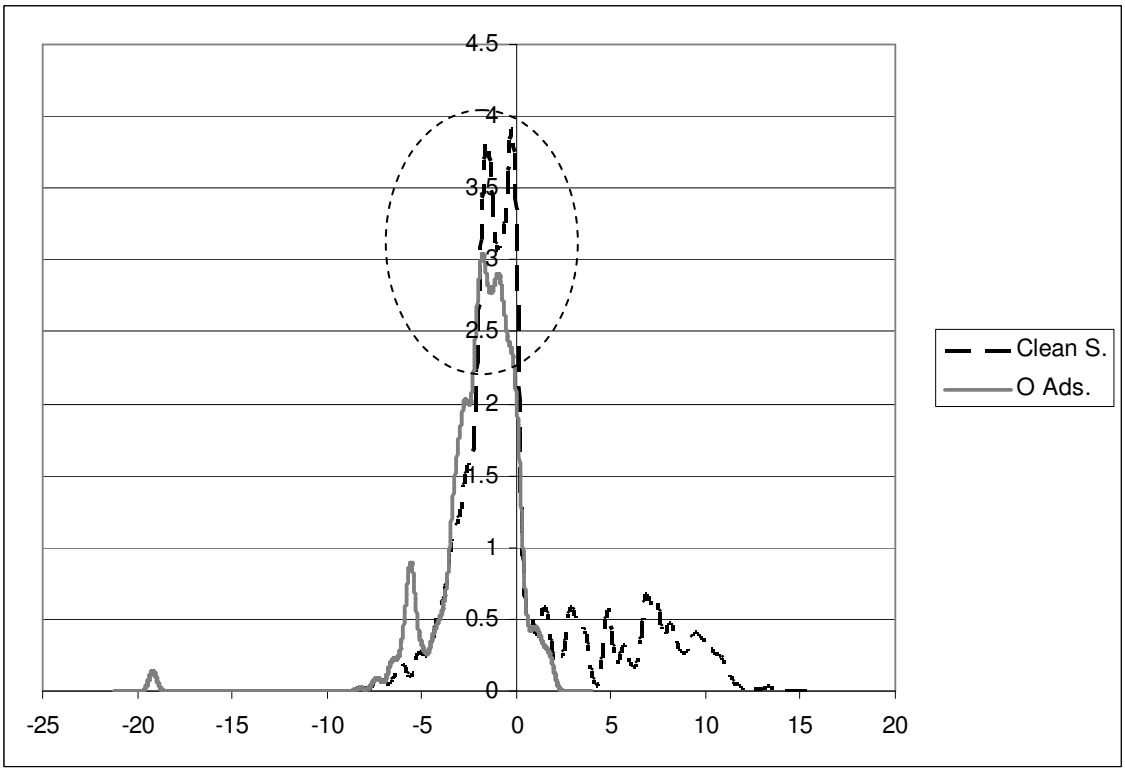


Figure 4.8. The LDOS profiles of Ni atom at 'Ni 5 layers' clean surface and at $fcc_{Ni3}$ site of oxygen adsorption on 'Ni 5 layers' surface

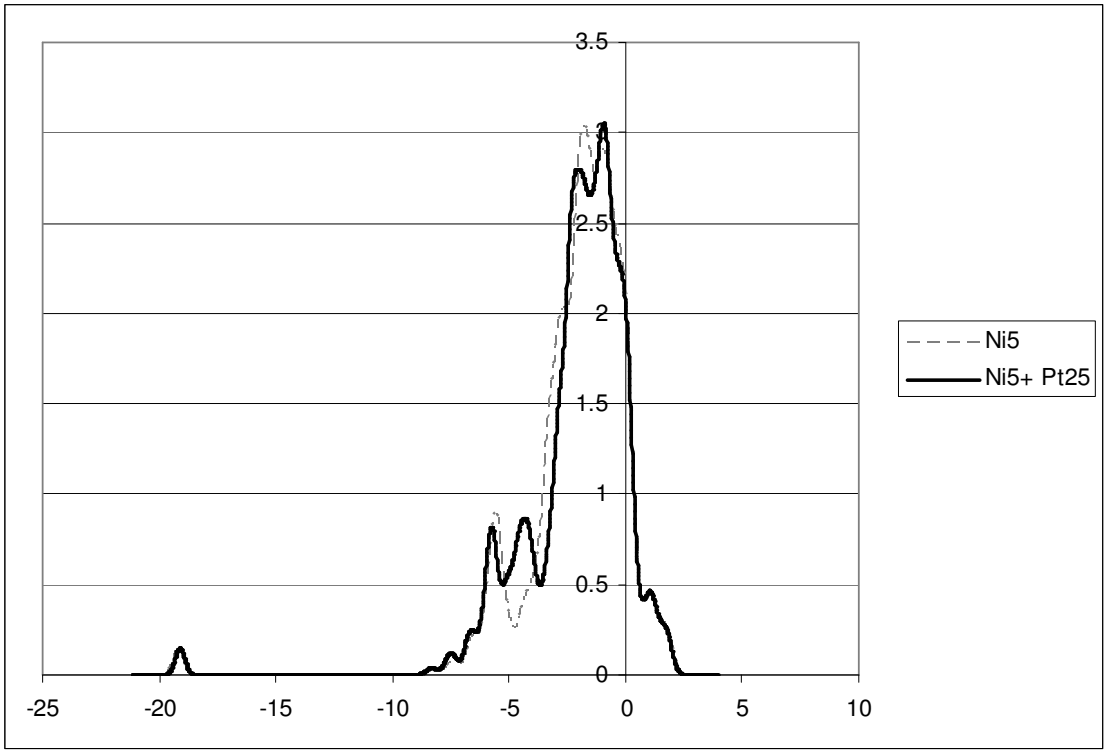


Figure 4.9. The LDOS profiles of Ni atom at $fcc_{Ni3}$ site of oxygen adsorption on 'Ni 5 layers' and 'Ni 5 layers containing 25 per cent Pt at 1$^{st}$ layer' surfaces

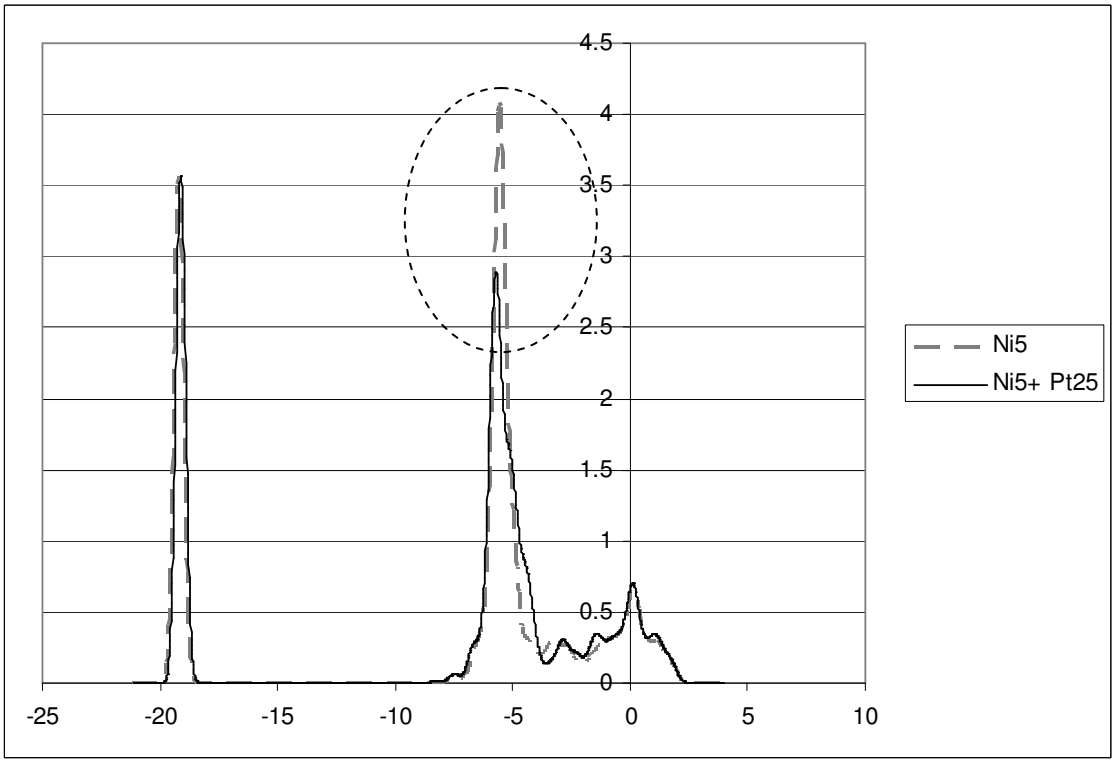


Figure 4.10. The LDOS profiles of O atom on 'Ni 5 layers' and 'Ni 5 layers containing 25 per cent Pt at 1$^{st}$ layer' surfaces

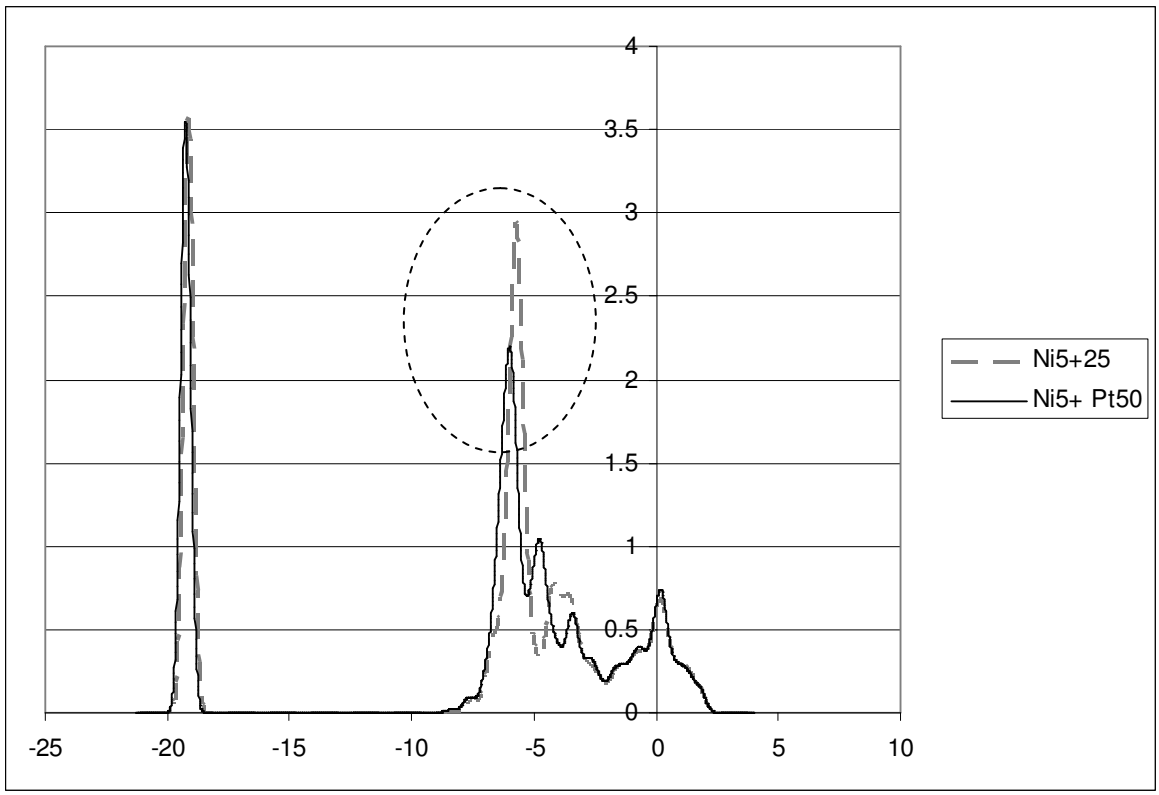


Figure 4.11. The LDOS profiles of O atom on 'Ni 5 layers containing 25 per cent Pt at 1st layer' and 'Ni 5 layers containing 50 per cent Pt at 1st layer'

### 4.2.2. Adsorption on Pseudomorphic Pt Layers on Ni

In this study, there were two different surface structures to be investigated in this section. One of the surfaces was created by depositing one layer of Pt on four layers of Ni and the other one was created by depositing two layers of Pt on three layers of Ni. It was explained in section 4.1.2 that; when topmost one or two layers of Ni layers were fully covered with Pt, the energy of surfaces were calculated as 2.37 J/m$^2$ for surface 'Ni 4 layers + Pt 1 layer' and 3.79 J/m$^2$ for surface 'Ni 3layers + Pt 2 layers', which can be seen in Figures 3.7 and Figure B.2, respectively. The results show that; since the clean surface energies of these surfaces were very high with respect to the other clean, stable surfaces, adsorption on 'Ni 4 layers + Pt 1 layer' and 'Ni 3layers + Pt 2 layers' surfaces was not expected "reasonable". It may also be noted that; the adsorption energy on surface 'Ni 4 layers + Pt 1 layer' was -3.75 eV and on 'Ni 3layers + Pt 2 layers' was -6.56 eV (from Table 4.5).

As shown in figures, these structures were deformed too much during the adsorption of oxygen atom. The probable reason for that was the size difference between Ni and Pt atoms. Ni has lattice parameters 5.00, 5.00, 20.17 Å and Pt has 5.55, 5.55, 21.06 Å. Large Pt atoms were compressed in small Ni lattice and too much stress caused the structures broke down.

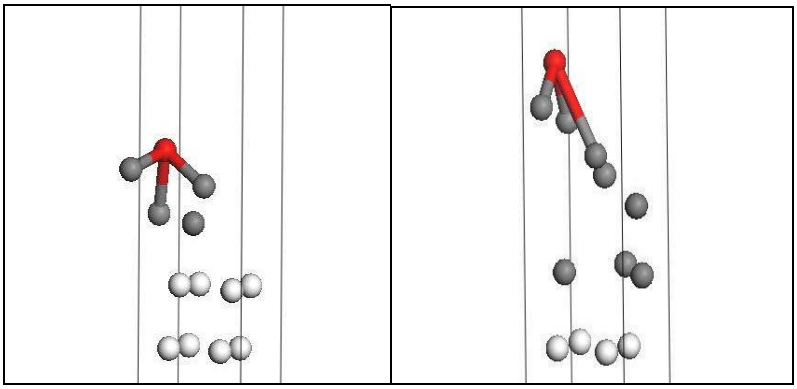

(a) (b)

Figure 4.12. Oxygen Adsorption on (a) 'Ni 4 layers + Pt 1 layer'
(b) 'Ni 3 layers + Pt 2 layers'
(○:Ni, ●: Pt, and the single atom at the top is oxygen atom)

When compared to the results in previous section including Pt-Ni surface alloys formed by substitutional adsorption, it can be concluded that; adsorption on 'Ni 4 layers + Pt 1 layer' and 'Ni 3layers + Pt 2 layers' did not give reasonable results. Since the increase in the number of Pt atoms resulted in compressive stress on structures containing high concentration of Pt atoms**,** which are larger than Ni atoms in size, the adsorption surfaces were deformed.

## 4.3. $CH_4$ Adsorption

In OSR reaction, as explained in the experimental papers before, steam reforming takes place on Ni sites and oxidation reaction is conducted on Pt sites. Endothermic steam reforming (on Ni site) absorbs the heat released from exothermic total oxidation (on Pt site). Thus, $CH_4$ adsorption is essential for both Pt and Ni sites.

$CH_4$ adsorption was studied on five different surfaces in this study; (i) 'Ni 5 layers', (ii) 'Ni 5 layers containing 25 per cent Pt at 1st layer', (iii) 'Ni 4 layers + Pt 1 layer', (iv)'Ni 3 layers and Pt 2 layers', and (v) 'Pt 2 layers'. The dissociative adsorption site for methane is the same for all those five surfaces; Figure 3.8 shows the adsorption site and Table 4.7 includes the data of methane adsorption energy. At the end of the simulations, the surfaces (iii) and (iv) with methane adsorbed on them were highly-deformed, especially surface containing two layers of platinum. The bond lengths became too longer than the original setup. This shows that these two structures are unstable and; -6.40 eV and 10.10 eV values cannot be taken into consideration because of this instability. One of the reasons of the instability may be the fact that substituted Pt atoms are stuck in the Ni lattice (like in adsorption of oxygen on pseudomorphic Pt layers). This affects the clean surface energy and once clean surface energy is changed, adsorption process is completely modified. The deformation of the fcc-methane adsorption site on 'Ni 4 layers + Pt 1 layer' is given in Figure 4.9 as an example.

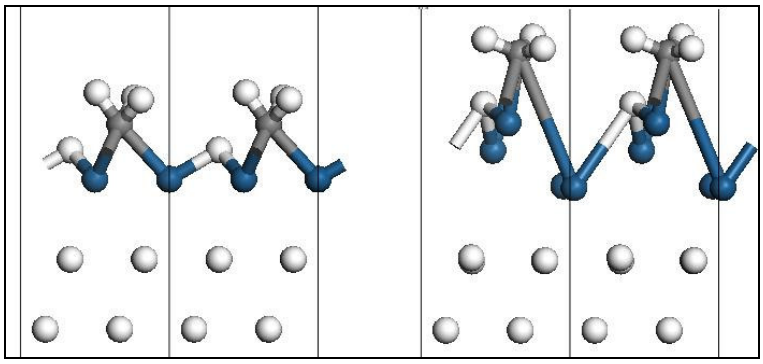

(a) (b)

Figure 4.13. Ni 4 Layers, Pt 1 Layer Surface (a) Before and (b) After $CH_4$ adsorption

On the other hand, the surfaces (i), (ii) and (v) were not deformed upon $CH_4$ adsorption significantly. Pure Ni surface has adsorption energy of -6.03 eV. It is clearly seen that, as the topmost layer is changed with substituting 25 per cent of Pt, the $CH_4$ adsorption energy value decreases and becomes -5.70 eV, which shows that the best catalyst surface for $CH_4$ adsorption based on adsorption energy 'Ni 5 layers containing 25 per cent Pt at 1st layer'. The minimum adsorption energy value for 5 Ni layers containing 25 per cent Pt at topmost layer means that this is the most suitable surface for $CH_4$ adsorption between the Ni-including surfaces. It should be noted that Pt 5 Layers has an

adsorption value of -6.24 eV which clearly shows that $CH_4$ adsorption is also favorable on monometallic Pt  The chart composed of comparable structures (Ni 5 layers, Ni 5 layers Pt 25 per cent at 1st layer, Ni 4 layers Pt1 layer) can be seen in Figure 4.14 below.

Table 4.6. Adsorption Energies of methane on monometallic and bimetallic Pt-Ni layers

| Surface Name | $E_A$ ($CH_4$) (eV) |
|---|---|
| 'Ni 5 layers' | -6.03 |
| 'Ni 5 layers containing 25 per cent Pt at 1st layer' | -5.70 |
| 'Ni 4 layers + Pt 1 layer' | -6.40 |
| 'Ni 3layers + Pt 2 layers' | -10.10 |
| 'Pt 5 layers' | -6.24 |

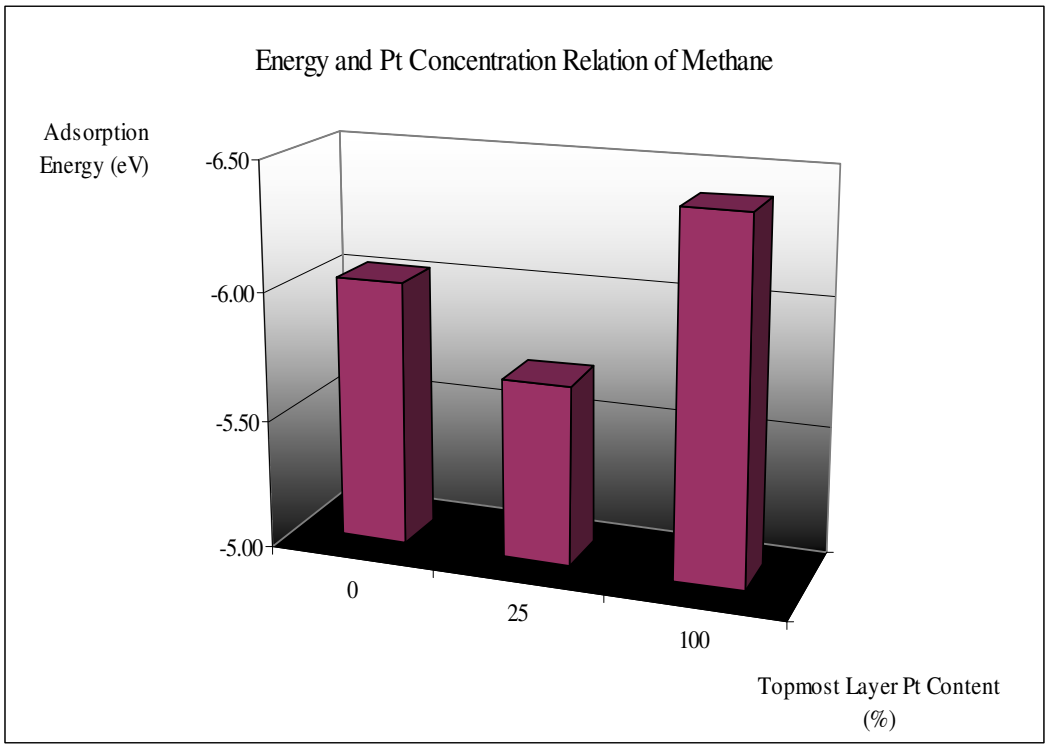


Figure 4.14. $CH_4$ Adsorption Energy Change with Pt Concentration at 1st Layer of 'Ni 5 Layers'

# 5. CONCLUSIONS

- For O adsorption, fcc, atop and hcp sites were stable, but bridge site was unstable. The comparison of the stable sites showed that the most energetically favored site for monometallic Ni(111) surface was fcc site.

- Clean surface energy data were analyzed to be used in adsorption energy calculations and the data showed that Pt presence on the Ni metal layers affected the adsorption properties of the surface. As the energy of the clean surface decreased, the stability of the clean surface increased and oxygen adsorption is weakened.

- The relationship between stability of clean surfaces and surface stress were examined. It was proven that, if Pt was added to the system the surface stress was decreased. The surface structure with a stress close to zero corresponds to lowest surface energy, i.e. the most stable surface structure. This is at 25 per cent Pt concentration of Pt-Ni surface alloy.

- For the same site (fcc), oxygen adsorption energy was dependent not only on the concentration of Pt in Ni, but also the number of Pt-O and Ni-O bonds.

- Energetically favored surface for oxygen adsorption was 75 per cent Pt deposited on the topmost layer of five layers of Ni atoms (F.75- O/$fcc_{Pt3}$); with the weakest O adsorption ($E_{ads}$: -2.72 eV). Over-stress caused surface deformation during adsorption at this surface structure.

- LDOS analysis of surface Ni atoms proved that there is electron transfer from Ni to Pt atoms. Decreased electron density on Ni atoms resulted in an increased work function at the surface. As O adsorption is based on electrostatic interaction, the decreased tendency of electron transfer from metal surface to O decreases the strength of O adsorption. LDOS analysis of O atom on metal surface also

confirmed that less electron charge is accumulated on the adsorbate when there is Pt on the metal surface.

- The best catalyst surface for $CH_4$ adsorption based on adsorption energy is 'Ni 5 containing 25 per cent Pt at 1$^{st}$ layer' with an adsorption energy of -5.70 eV. The weakest adsorption energy for 5 Ni layers containing 25 per cent Pt at topmost layer means that this is the most suitable surface for $CH_4$ adsorption between the Ni-including surfaces. It should be noted that Pt 5 Layers has an adsorption value of -6.24 which clearly shows that $CH_4$ adsorption is also favorable on monometallic Pt.

# 6. RECOMMENDATIONS

Considering the results obtained in this study, following ideas are suggested for future studies: (i) Methane adsorption sites might be changed. (ii) Methane adsorption can be analyzed on different types of Pt-Ni surfaces, containing different Pt concentrations. (iii) Co-adsorption of OSR reactants, i.e. water and methane, and methane and oxygen might be tried on various Pt-Ni surfaces as well as monometallic Pt and Ni; and the results obtained may be relatively analyzed. (iv) Reaction pathways analysis can be performed on various Pt-Ni surfaces for SR and TOX.

# APPENDIX A: WORK FUNCTION CHARTS

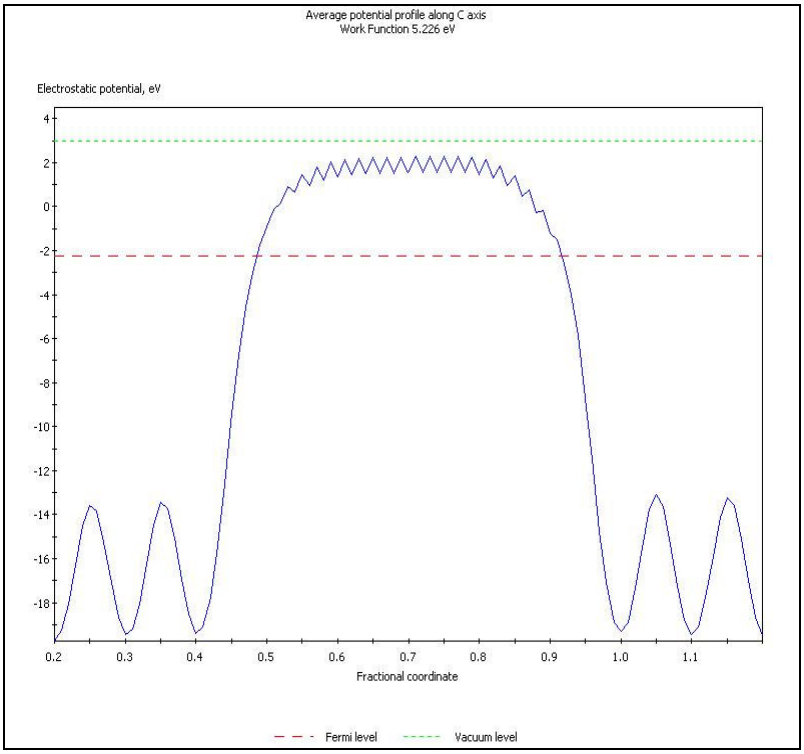


Figure A. 1. Work function chart for 'Ni 5 layers' surface

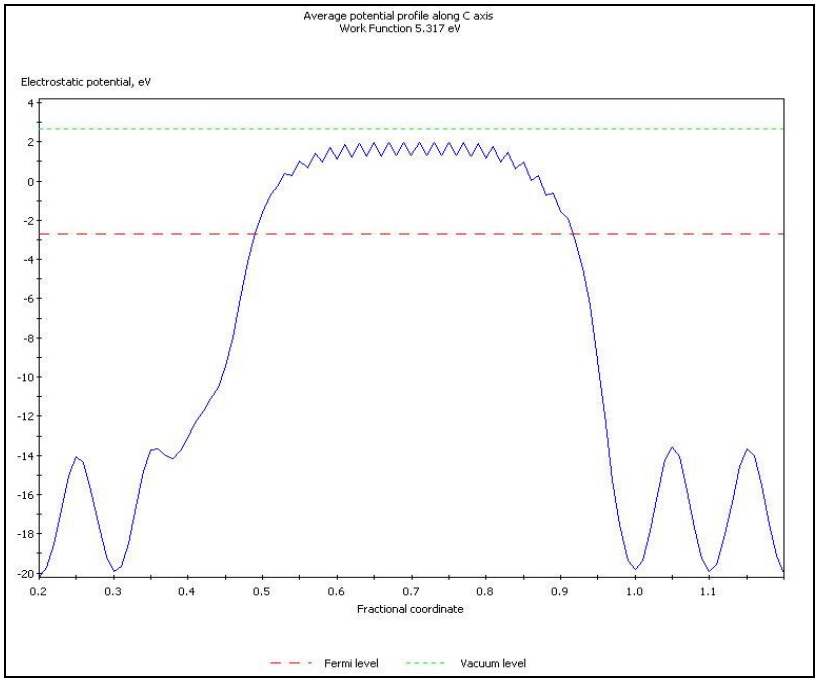


Figure A. 2. Work function chart for 'Ni 5 layers containing 25 per cent Pt at 1st layer' surface

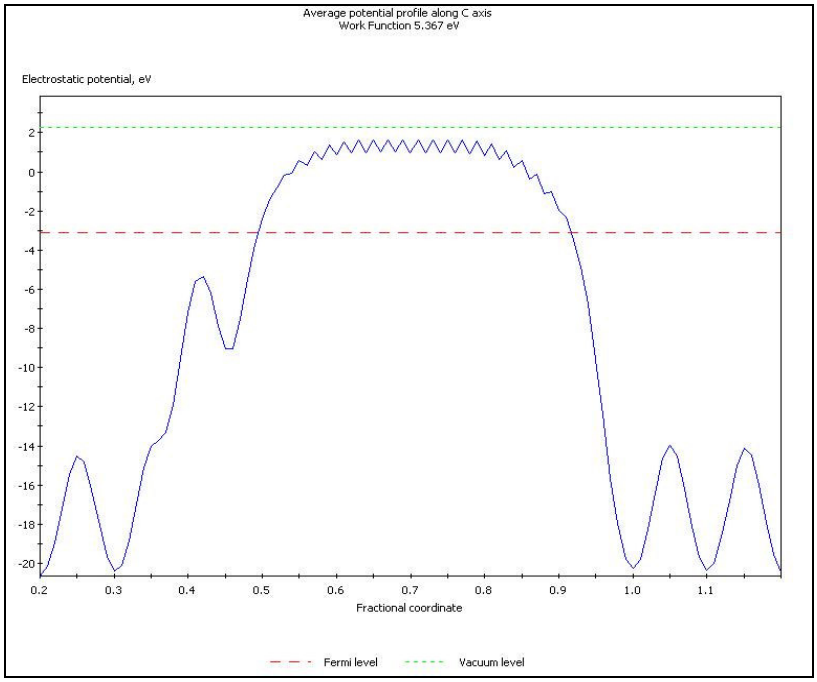


Figure A. 3. Work function chart for 'Ni 5 layers containing 50 per cent Pt at 1st layer' surface

# APPENDIX B: SURFACE STRUCTURES

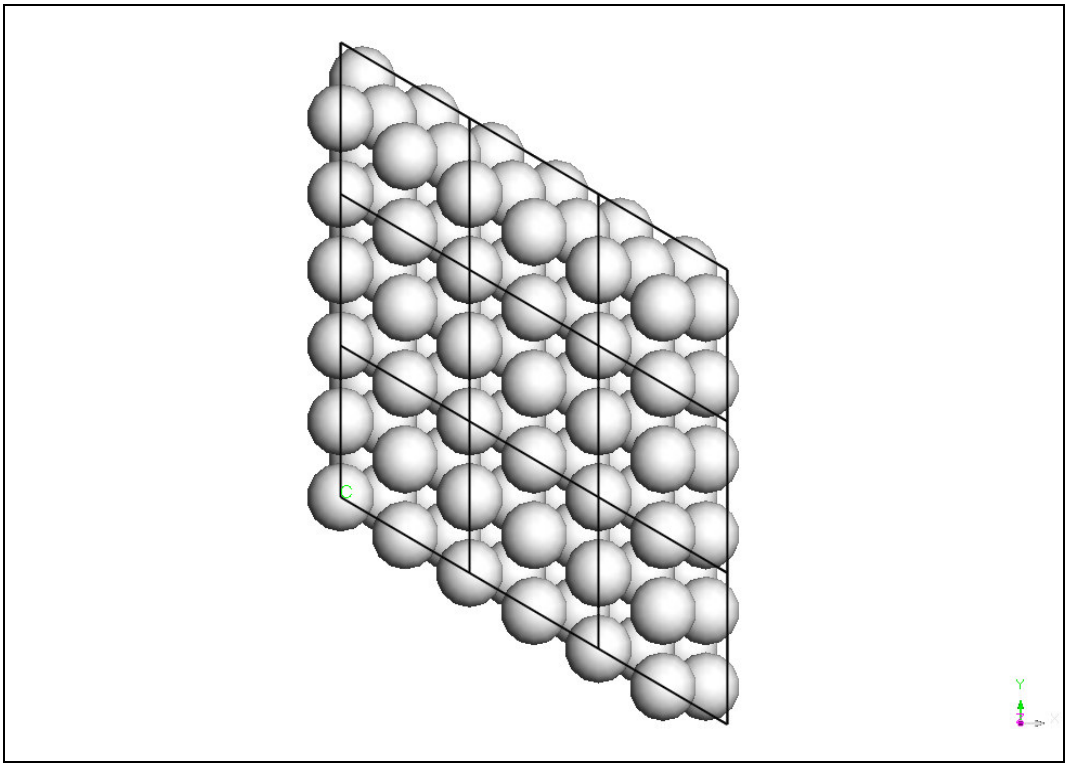

Figure B. 1. 'Ni 5 layers" Pure Ni

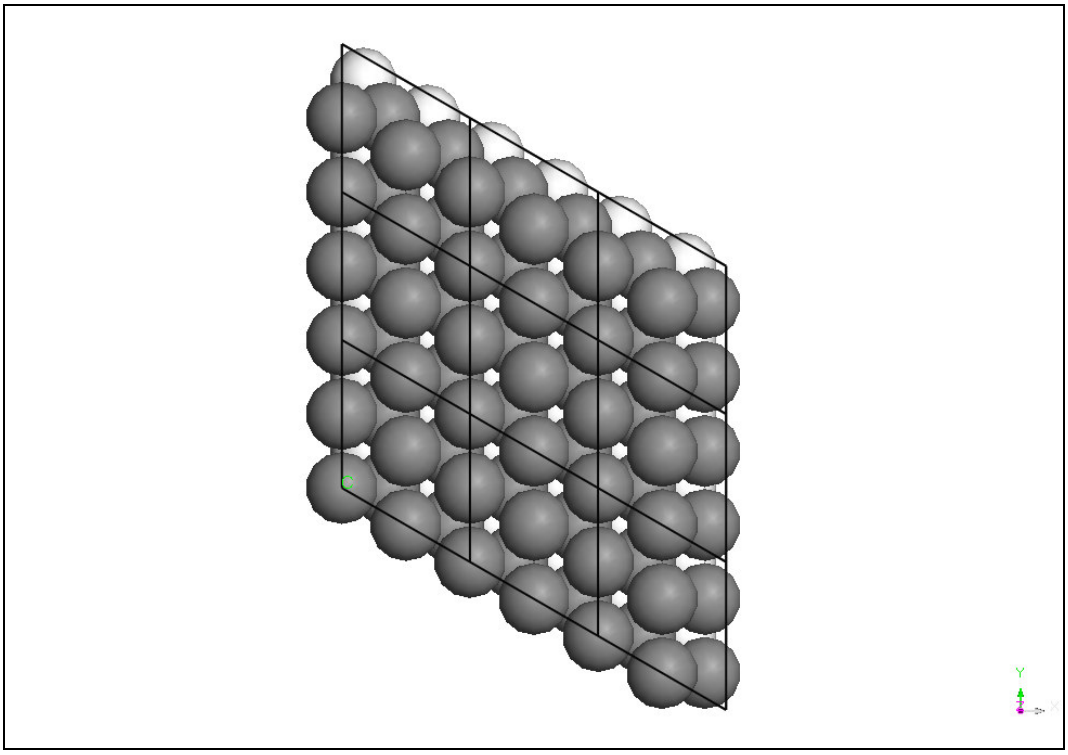

Figure B. 2. 'Ni 3 layers + Pt 2 layers'

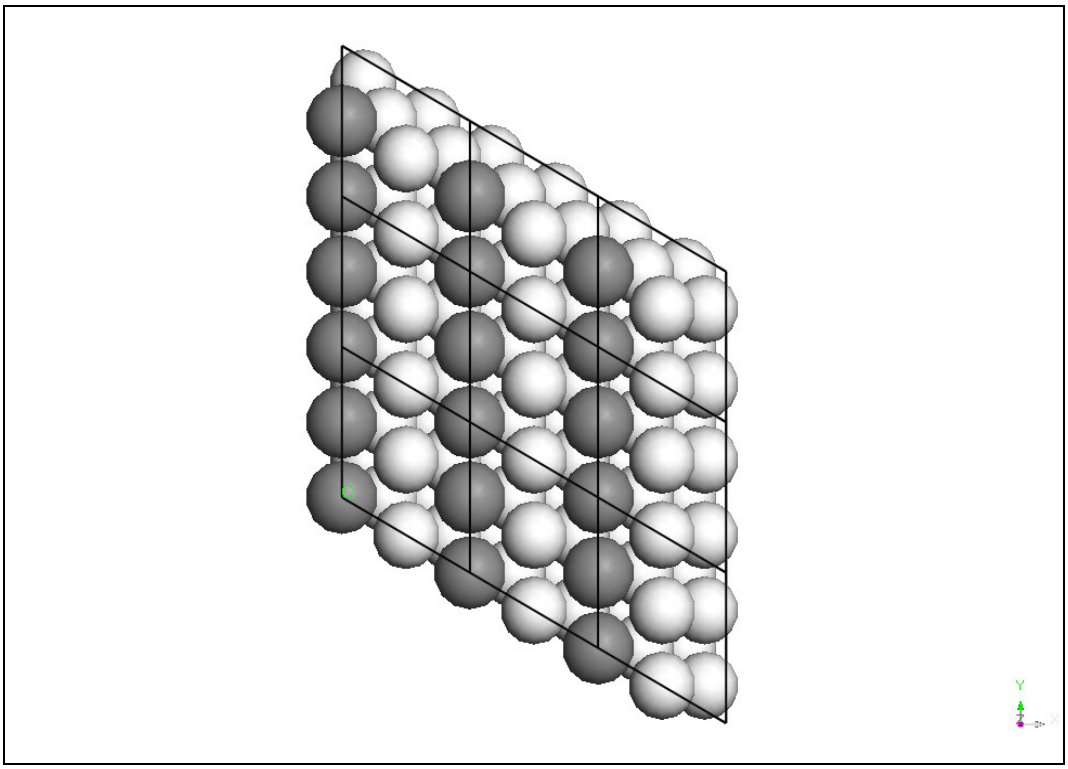

Figure B. 3. 'Ni 5 layers containing 50 per cent Pt at 1$^{st}$ layer'

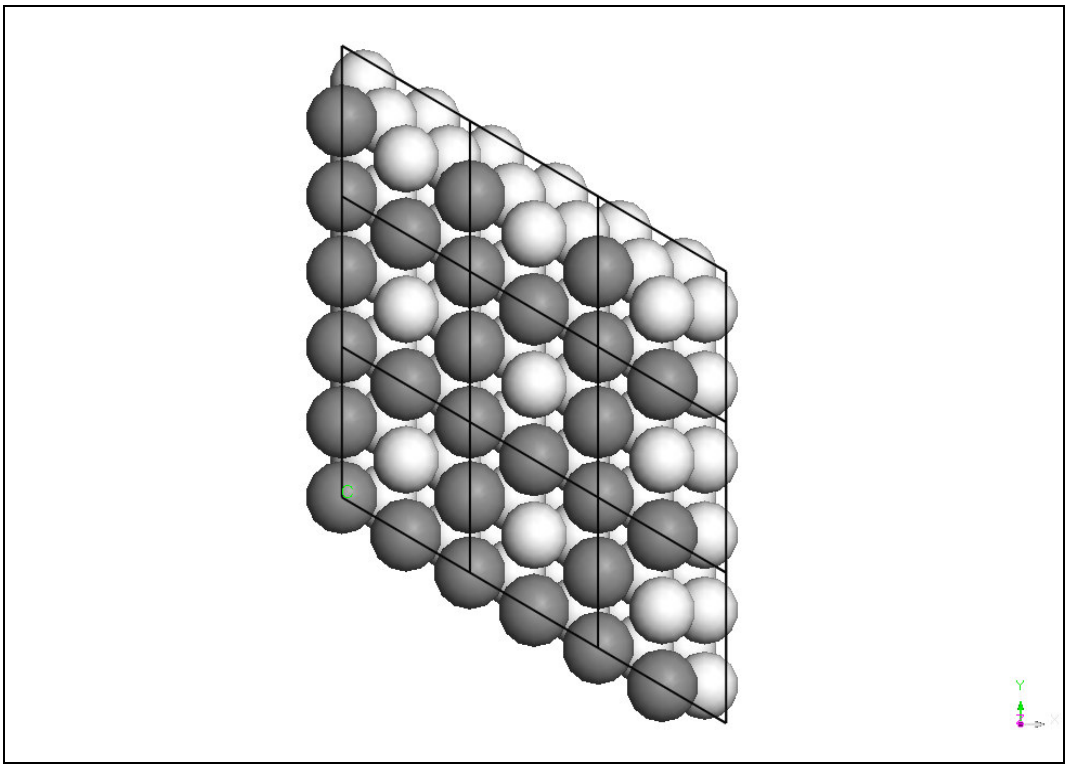

Figure B. 4. 'Ni 5 layers containing 75 per cent Pt at 1st layer'

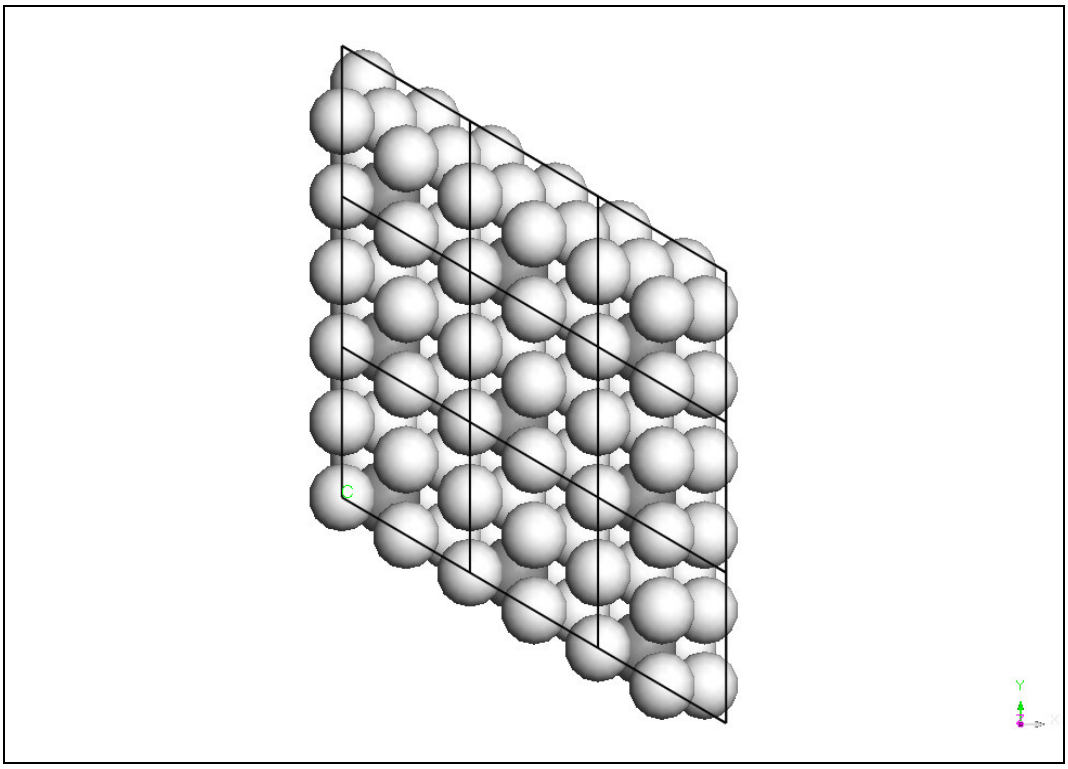

Figure B. 5. 'Ni 5 layers containing 25 per cent Pt at 2nd layer'

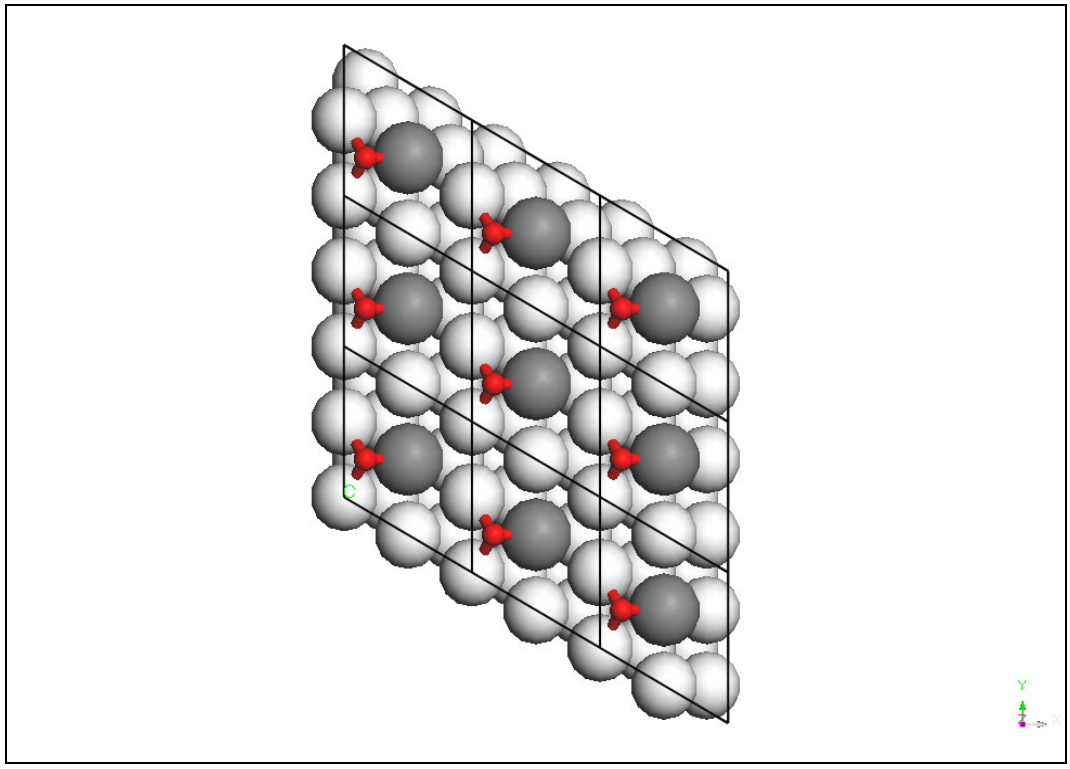

Figure B. 6. 'Ni 5 layers containing 25 per cent Pt at 1st layer' - O/$fcc_{Ni2Pt1}$

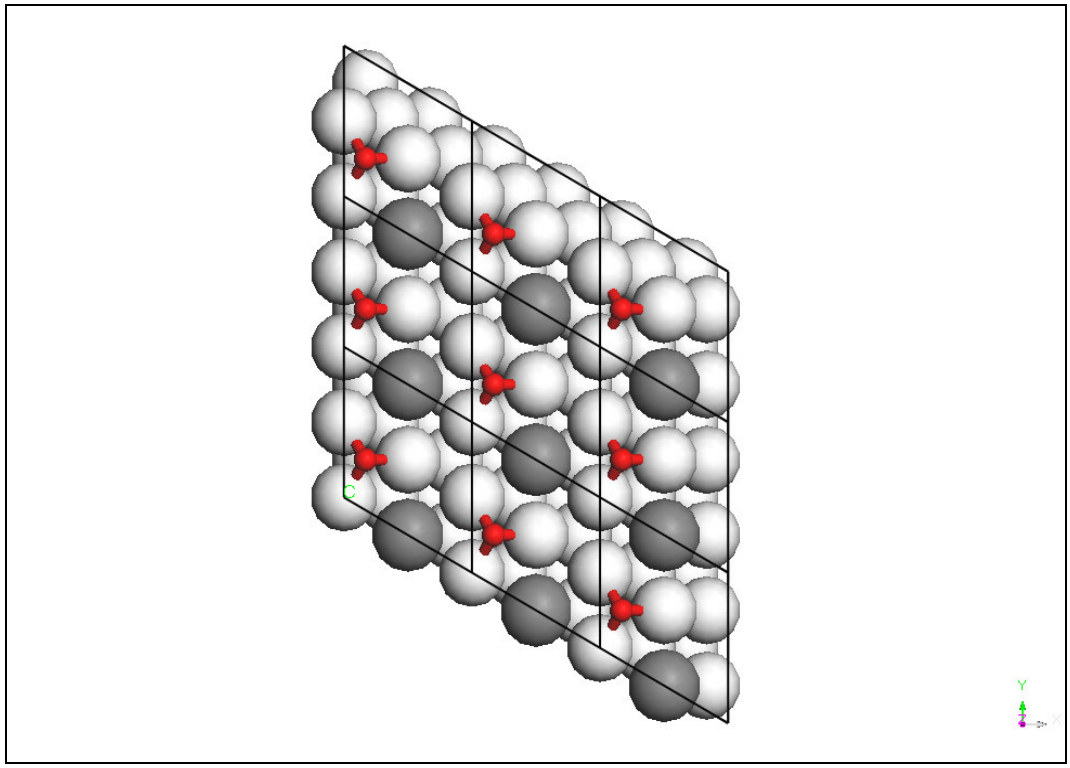

Figure B. 7. 'Ni 5 layers containing 25 per cent Pt at 1st layer' - O/$fcc_{Ni3}$

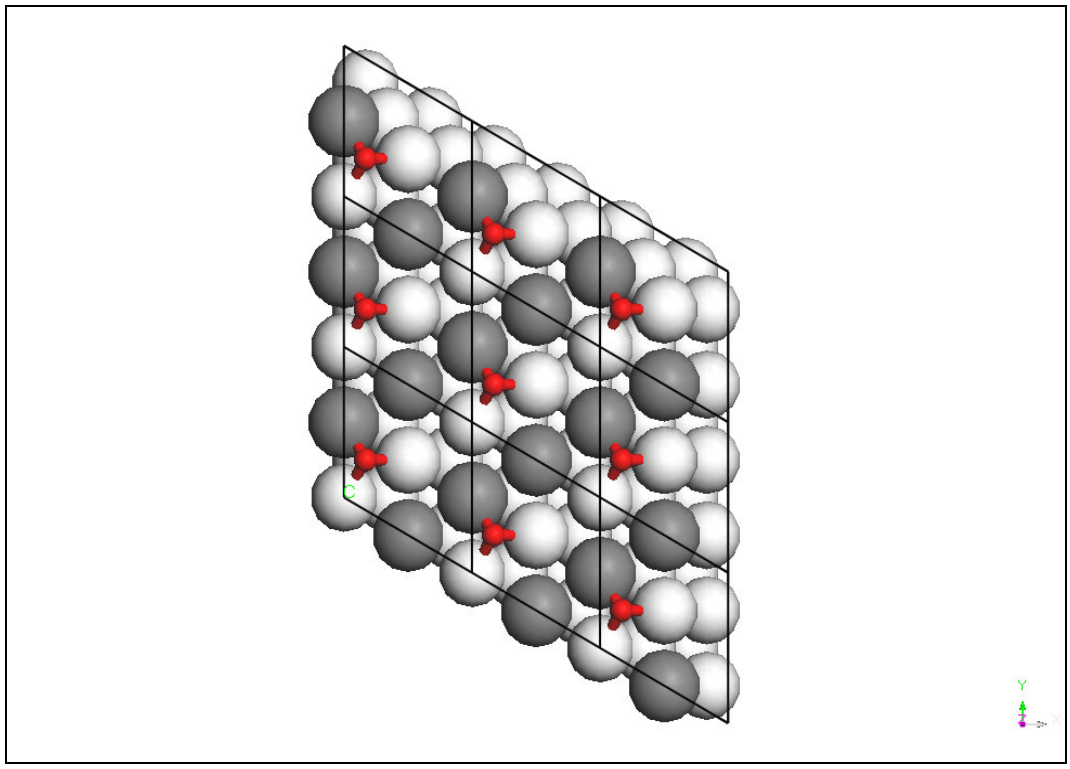

Figure B. 8. 'Ni 5 layers containing 50 per cent Pt at 1st layer' - O/fcc$_{Ni2Pt1}$

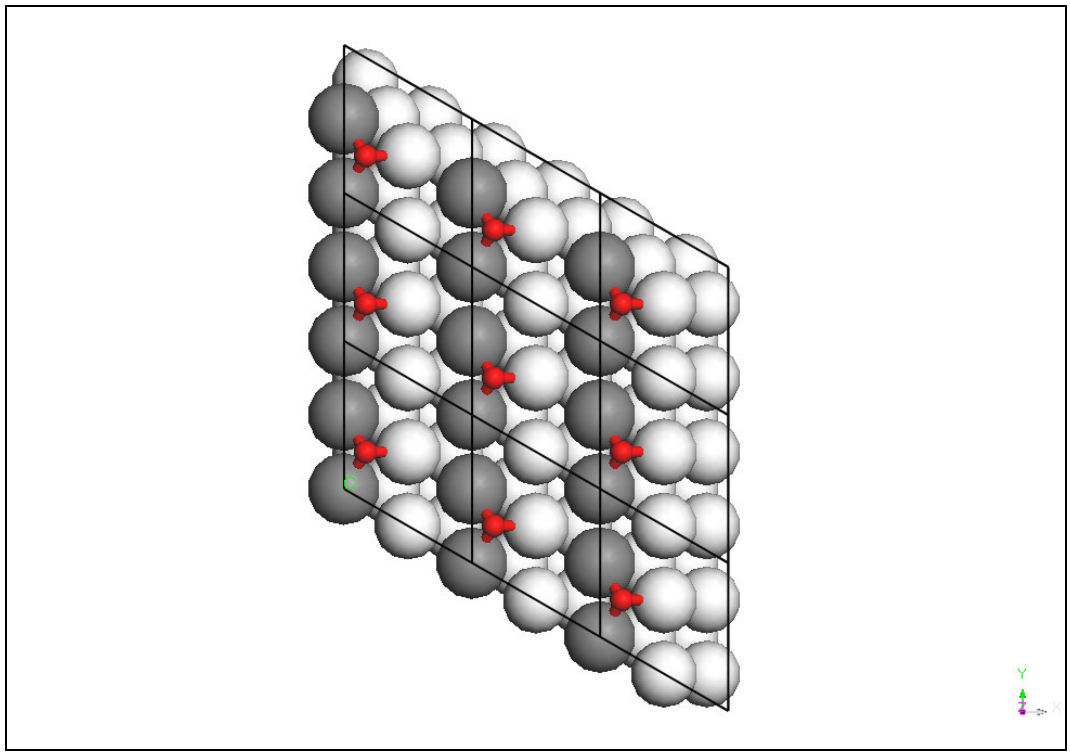

Figure B. 9. 'Ni 5 layers containing 50 per cent Pt at 1st layer' - O/fcc$_{Ni1Pt2}$

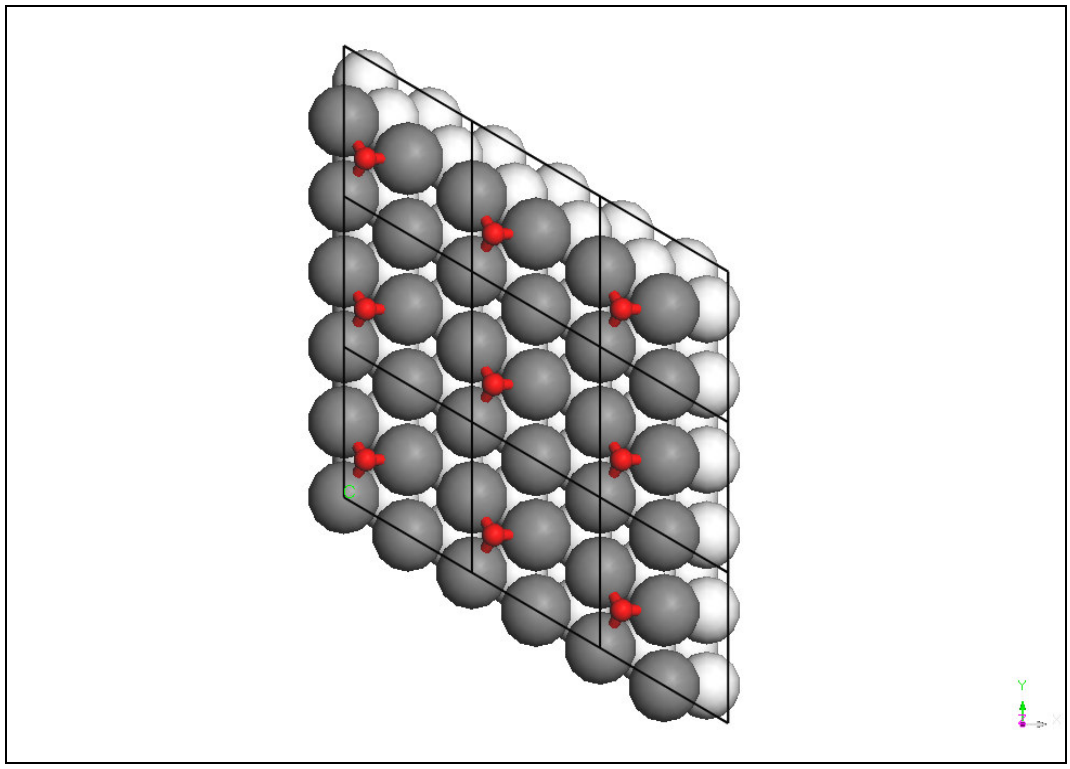

Figure B. 10. 'Ni 4 Layers + Pt 1 layer' - O/$fcc_{Pt3}$

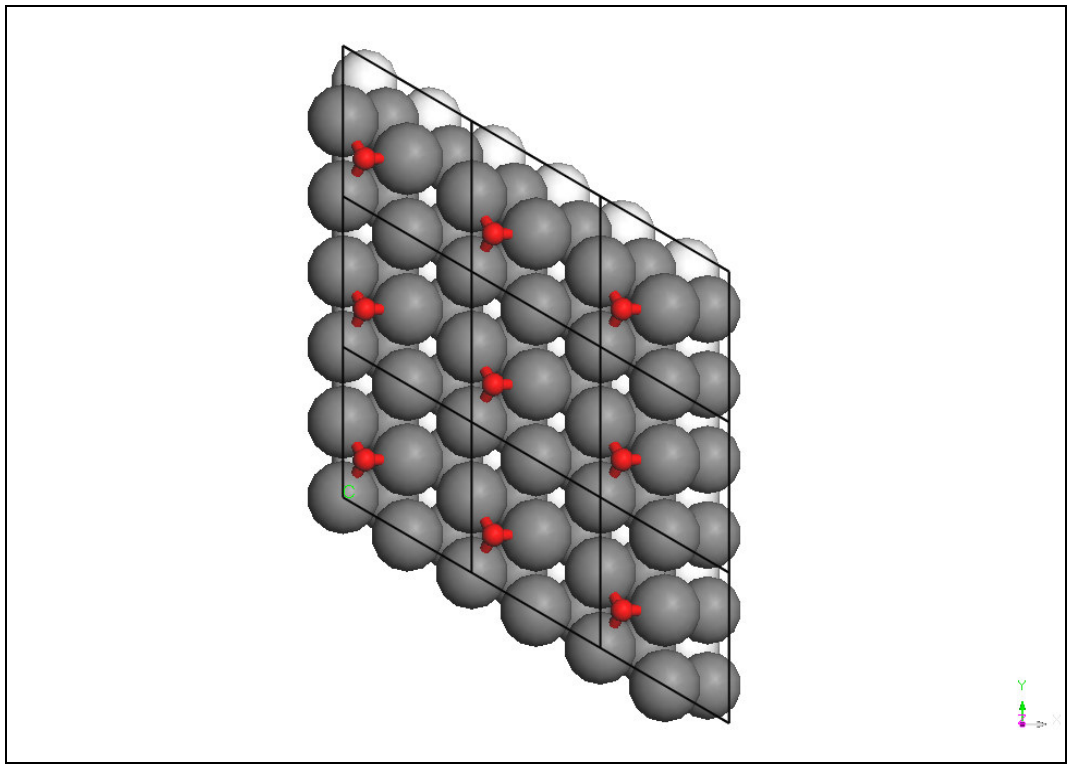

Figure B. 11. 'Ni 3 Layers + Pt 2 layers' O/$fcc_{Pt3}$

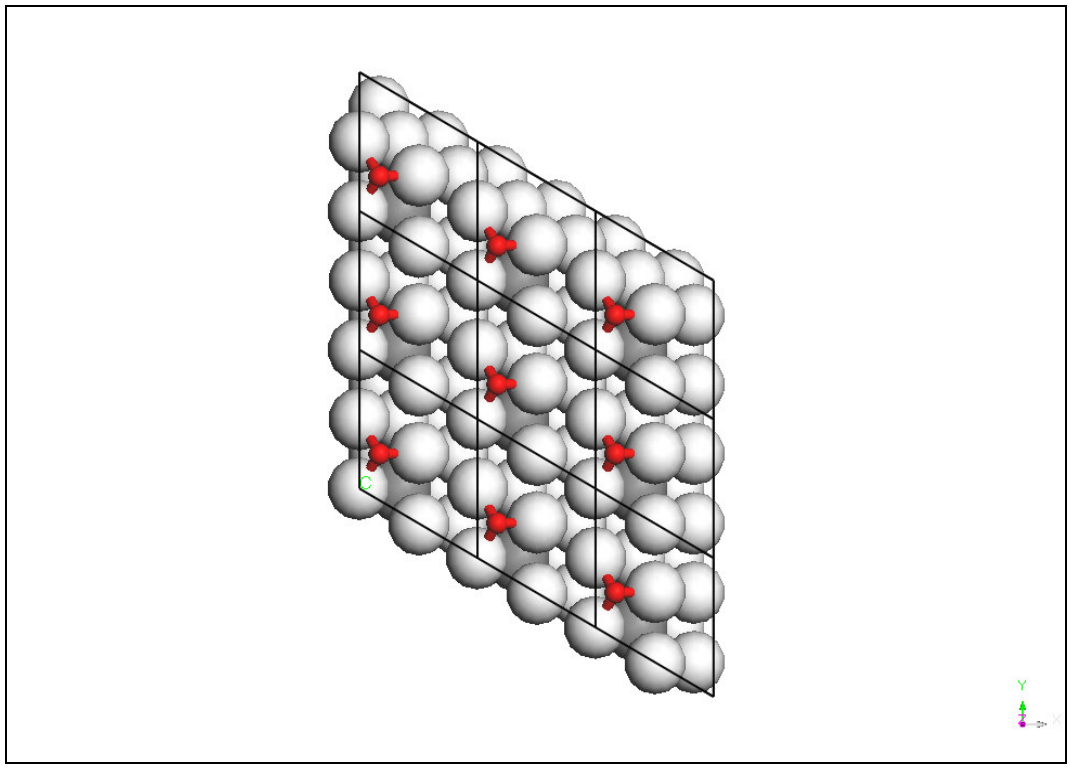

Figure B. 12. 'Ni 5 layers containing 25 per cent Pt 2nd layer' - O/fcc$_{Ni3}$

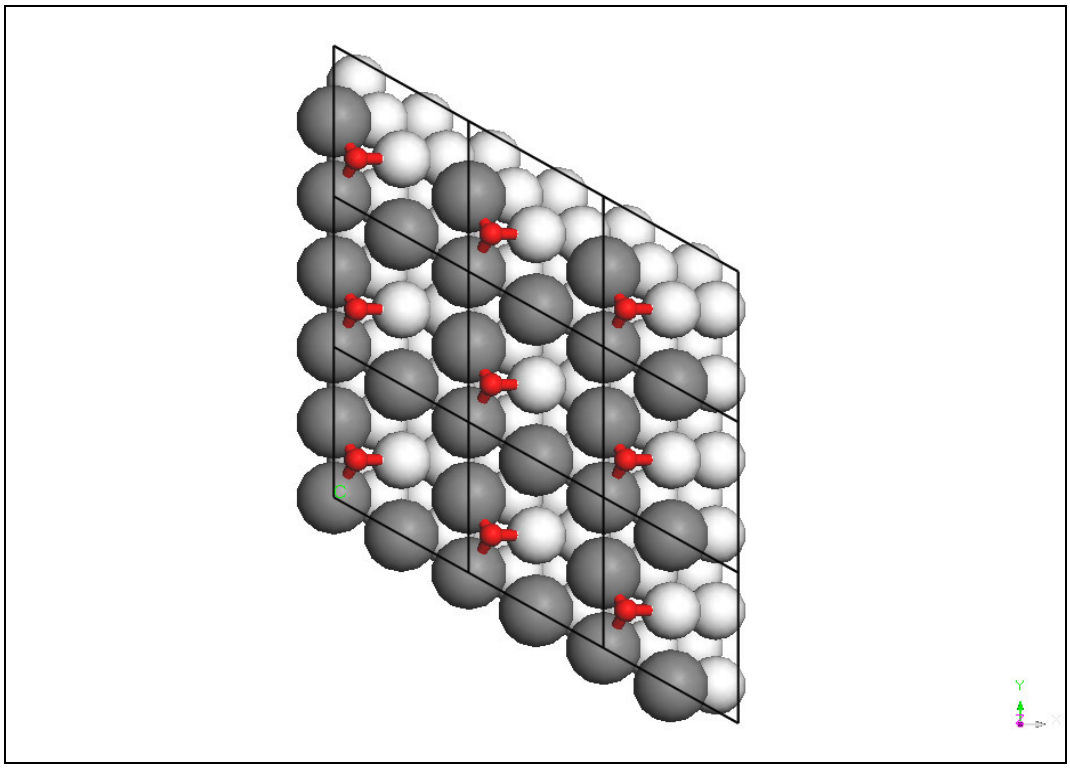

Figure B. 13. 'Ni 5 layers containing 75 per cent Pt at 1st layer' - O/fcc$_{Ni1Pt2}$

# REFERENCES


1. Wu, S. J., S. W. Shiah and W. L. Yu, "Parametric Analysis of Proton Exchange Membrane Fuel Cell Performance by Using the Taguchi Method and a Neural Network", *Renewable Energy*, Vol. 34, pp. 35-144, 2009.

2. Tan, Ö., E. Maşalacı, Z. İ. Önsan and A. K. Avcı, "Design of a Methane Processing System Producing High-Purity Hydrogen", *International Journal of Hydrogen Energy*, Vol. 33, pp. 5516-5526, 2008.

3. Sümer, A., M. A. Gülmen and A. E. Aksoylu, "A Theoretical Investigation on $Pt_3Sn$ (102) Surface Alloy and CO-$Pt_3Sn$ (102) System", *Surface Science*, Vol. 600, pp. 2026-2039, 2006.

4. Gökaliler, F., B. S. Çağlayan, Z. İ. Önsan and A. E. Aksoylu, "Hydrogen Production by Autothermal Reforming of LPG for PEM Fuel Cell Applications", *International Journal of Hydrogen Energy*, Vol. 3, pp. 1383-1391, 2008.

5. Trimm, D. L. and Z. İ. Önsan, "Onboard Fuel Conversion for Hydrogen-Fuel-Cell-Driven Vehicles", *Catalysis Reviews*, Vol. 43, pp. 31-84, 2001.

6. Çağlayan, B. S., A. K. Avcı, Z. İ. Önsan and A. E. Aksoylu, "Production of Hydrogen Over Bimetallic Pt-Ni/δ-$Al_2O_3$ I. Indirect Partial Oxidation of Propane", *Applied Catalysis A: General*, Vol. 280, pp. 181-188, 2005.

7. Çağlayan, B. S., Z. İ. Önsan and A. E. Aksoylu, "Production of Hydrogen over Bimetallic Pt-Ni/δ-$Al_2O_3$: II. Indirect Partial Oxidation of LPG", *Catalysis Letters*, Vol. 102, pp. 63-67, 2005.

8. Örücü, E., F. Gökaliler, A. E. Aksoylu and Z. İ. Önsan, "Ethanol Steam Reforming for Hydrogen Production over Pt-Ni/δ-$Al_2O_3$", *Catalysis Letters*, Vol. 120, pp. 193-203, 2008.

9. Ahmet, S. and M. Krumpelt, "Hydrogen from Hydrocarbon Fuels for Fuel Cells", *International Journal of Hydrogen Energy,* Vol. 26, pp. 291-301, 2001.

10. Fuel Cell Today (FC Today-X), http://www.fuelcelltoday.com/reference/faq, 2008.

11. Özkara Ş. and A. E. Aksoylu, "Selective Low Temperature Carbon Monoxide Oxidation in $H_2$-Rich Gas Streams over Activated Carbon Supported Catalysts", *Applied Catalysis A: General*, Vol. 251, pp. 75-83, 2003.

12. Avcı A.K., D.L. Trimm, A.E. Aksoylu and Z.İ. Önsan, "Hydrogen Production by Steam Reforming of N-butane over Supported Ni and Pt-Ni catalyst", *Applied Catalysis*, Vol. 258, pp 235-240, 2004.

13. Karakaya, M., A. K. Avcı, A. E. Aksoylu and Z. İ. Önsan, "Steady-State and Dynamic Modeling of Indirect Partial Oxidation of Methane in a Wall-Coated Microchannel", *Catalysis Today*, Vol. 139, pp. 312-321, 2009.

14. Li, B., S. Kado, Y. Mukainakano, T. Miyazawa, T. Miyao, S. Naito, K. Okumura, K. Kunimori and K. Tomishige, "Surface Modification of Ni Catalysts with Trace Pt for Oxidative Steam Reforming of Methane", *Journal of Catalysis*, Vol. 245, pp. 144-155, 2007.

15. Sehested, J., J. A. P. Gelten, I. N. Remediakis, H. Bengaard and J. K. Nørskov, "Sintering of Nickel Steam-Reforming Catalysts: Effects of Temperature and Steam and Hydrogen Pressures", *Journal of Catalysis*, Vol. 223, pp. 432-443, 2004.

16. Mukainakano, Y., S. Kado, K. Okumura, K. Kunimori and K. Tomishige, "Catalytic Performance and Characterization of Pt–Ni Bimetallic Catalysts for Oxidative Steam Reforming of Methane", *Chemical Engineering Science*, Vol. 63, pp. 4891-4901, 2008.

17. Yoshida, K., K. Okumura, T. Miyao, S. Naito and K. Tomishige, "Oxidative Steam Reforming of Methane over Ni/α-$Al_2O_3$ Modified with Trace Pd", *Applied Catalysis A: General*, Vol:351, pp. 217-225, 2008.

18. Tomishige, K., S. Kanazawa, K. Ikushima and K. Kunimori, "Catalyst Design of Pt Modified Ni/$Al_2O_3$ Catalyst with Flat Temperature Profile in Methane Reforming with $CO_2$ and $O_2$", *Catalysis Letters*, Vol. 84, pp. 69-74, 2002.

19. Tomishige, K., S. Kanazawa, S. Ito and K. Kunimori, "Catalyst development for direct heat supply from combustion to reforming in methane reforming with $CO_2$ and $O_2$", *Applied Catalysis A: General*, Vol. 244, pp 71-82, 2003.

20. Li, B., S. Kado, Y. Mukainakano, M. Nurunnabi, T. Miyao, S. Naito and K. Tomishige, "Temperature Profile of Catalyst Bed During Oxidative Steam Reforming of Methane over Pt-Ni Bimetallic Catalysts", *Applied Catalysis A: General*, Vol. 304, pp 62-71, 2006.

21. Mukainakano, Y., B. Li, S. Kado, T. Miyazawa, S. Naito, K. Kunimori, and K. Tomishige, "Surface Modification of Ni Catalysts with Trace Pd and Rh for Oxidative Steam Reforming of Methane", *Applied Catalysis A: General,* Vol. 318, pp. 252-264, 2007.

22. Mukainakano, Y., K. Yoshida, K. Okumura, K. Kunimori and K. Tomishige, "Catalytic Performance and QXAFS Analysis of Ni Catalysts Modified with Pd for Oxidative Steam Reforming of Methane", *Catalysis Today*, Vol. 132, pp. 101-108, 2008.

23. Nikolla, E., J. W. Schwank and S. Linic, "Hydrocarbon Steam Reforming on Ni Alloys at Solid Oxide Fuel Cell Operating Conditions", Catalysis Today, Vol. 136, pp. 243-248, 2008.

24. Lischka, M. C. Mosch and A. Groß, "Tuning Catalytic Properties of Bimetallic Surfaces: Oxygen Adsorption on Pseudomorphic Pt/Ru Overlayers", *Electrochimica Acta*, Vol. 52, pp. 2219-2228, 2007.

25. Gülmen, M., A. Sümer and A. E. Aksoylu, "Adsorption Properties of CO on Low-index $Pt_3Sn$ Surfaces", *Surface Science*, Vol. 600, pp. 4909-4921, 2006.

26. Wang, S. G., X. Y. Liao, J. Hu, D. B. Cao, Y. Li, J. Wang, H. Jiao, "Kinetic Aspect of $CO_2$ reforming of $CH_4$ on Ni(111): A Density Functional Theory Calculation", *Surface Science*, Vol. 601, pp. 1271-1284, 2007.

27. Cabeza, G. F., N. J. Castellani and P. Legare, "Adhesion and Bonding of Pt/Ni and Pt/Co Overlayers: Density Functional Calculations", *Journal of Physics and Chemistry of Solids*, Vol. 67, 690-697, 2006.

28. Yamagashi, S., S. J. Jenkins, D.A. King, "First Principles Studies of Chemisorbed O on Ni{1 1 1}", *Surface Science*, Vol. 543, pp. 12-18, 2003.

29. Ma, Y. and P. B. Balbuena, "Pt Surface Segregation in Bimetallic $Pt_3M$ Alloys: A Density Functional Theory Study", *Surface Science*, Vol. 602, pp. 107-113, 2008.

30. Chen, M., S. P. Bates, R. A. Van Santen and C.M. Friend, "The Chemical Nature of Atomic Oxygen Adsorbed on Rh(111) and Pt(111): A Density Functional Study", *The Journal of Physical Chemistry*, Vol. 101, pp. 10051-10057, 1997.